DEVELOPMENT OF A HIGH THROUGHPUT CELL-BASED ASSAY TO SCREEN FOR INHIBITORS OF HIV-1 VPR OLIGOMERIZATION

by

Courtney Ann Zych

B.S., Biology, University of Texas at Austin, 2008

B.A., Humanities, University of Texas at Austin, 2008

Submitted to the Graduate Faculty of

the Department of Infectious Diseases and Microbiology

the Graduate School of Public Health in partial fulfillment

of the requirements for the degree of

Master of Science

University of Pittsburgh

2011

UNIVERSITY OF PITTSBURGH

GRADUATE SCHOOL OF PUBLIC HEALTH

This thesis was presented

by

Courtney Zych

It was defended on

April 13, 2011

and approved by

Thesis Advisor
Velpandi Ayyavoo, PhD
Associate Professor
Infectious Diseases and Microbiology
Graduate School of Public Health
University of Pittsburgh

Committee Member
Tianyi Wang, PhD
Assistant Professor
Infectious Diseases and Microbiology
Graduate School of Public Health
University of Pittsburgh

Committee Member
Yuan Pu Di, PhD
Assistant Professor
Environmental and Occupational Health
Graduate School of Public Health
University of Pittsburgh

Velpandi Ayyavoo, PhD

DEVELOPMENT OF A HIGH THROUGHPUT CELL-BASED ASSAY TO SCREEN FOR INHIBITORS OF HIV-1 VPR OLIGOMERIZATION

Courtney Zych, M.S.

University of Pittsburgh, 2011

Highly active anti-retroviral treatment (HAART) targets less than a third of the proteins produced during HIV-1 infection. Testing the effectiveness of an anti-retroviral drug requires assays specific for the individual target that take into account its mechanism of action. Most HIV-1 proteins need to undergo dimerization in order to become functional in the viral life cycle. Historically, it has been difficult to visualize and quantify changes in a protein-protein interaction, which has left this characteristic of proteins unexplored as potential antiviral targets. In this study, a bimolecular fluorescence complementation based screening assay is developed that can quantify a change in dimerization, using the HIV-1 accessory protein Vpr as a "proof of concept".

Results demonstrated that bimolecular fluorescence complementation of Vpr could be competed off in a dose-dependent manner using untagged, full length Vpr as a competitor molecule. The change in signal intensity was measured quantitatively through flow cytometry and fluorescence microscopy in a high content screening assay. High content imaging was used to screen a library of peptides and a library of small molecules for an effect on Vpr dimerization. None of the Vpr peptides were shown to have an effect; however, one of the small molecules was shown to interfere with Vpr dimerization in a dose-dependent manner.

Statement of Public Health relevance: Dimerization is a unique property of many HIV-1 viral proteins and is necessary to complete the viral life cycle, thus it has been identified as a potential drug target. By developing an assay that screens for inhibition of HIV-1 protein dimerization, high throughput screening can be performed to detect inhibitors of a new target in HIV-1 replication. Small molecules identified using this screening method could be developed into a novel anti-retroviral drug.

TABLE OF CONTENTS

LIST OF TABLES

LIST OF FIGURES

ACKNOWLEDGEMENTS

I would like to first thank Dr. Velpandi Ayyavoo, whose guidance has allowed me to transition from my background in diagnostic bacteriology to molecular virology. Her hands-on mentoring has taught me not only the fundamentals of research, but also how to manage the day-to-day functions of a laboratory. With her support, I have been granted innumerable opportunities to grow both as a student as well as a scientist. I would next like to thank Dr. Tianyi Wang and Dr. Peter Di, who have supported my thesis project with such encouragement and guidance. Their insights into my project's strengths and weaknesses were invaluable.

I could not have done any of this without the support and friendship of my fellow lab members. Their support and encouragement were instrumental in cultivating my positive attitude toward research. I hope that I have had the same positive effect on their outlook on the research profession. I would like to thank Pruthvi and Kevin, my fellow night owls, for burning the midnight oil alongside me and making incubations seem to fly by.

I would like to extend my gratitude to Willie Buchser of the University of Pittsburgh Cancer Institute Cytometry facility for his assistance with the high content imaging data analysis. His patience and willingness to work with me to obtain the clearest results were instrumental in the success of my screening. I would also like to thank LuAnn and the staff of the IDM flow

cytometry lab for putting up with me using their cytometers for hours on end and for trusting me to take apart their expensive machines, fix a problem, and put them back together again. Their patience, even in the face of technical difficulties, was heartening.

Finally, I would like to thank the department of Infectious Diseases and Microbiology and all the faculty, students and staff for their advice and encouragement throughout my studies. Everyone in the department has been exceptionally helpful, especially when I went looking for input on techniques or "just a tiny bit" of reagent. Whether I went looking for lab advice or life advice, I was always met with a friendly face. This open attitude is what first drew me to the IDM program at the Graduate School of Public Health, and I am lucky to have been able to earn my masters degree in a department with such warm and friendly people.

1.0 INTRODUCTION

1.1 THE AIDS EPIDEMIC

There are currently an estimated 33.3 million people infected worldwide with HIV/AIDS (Human Immunodeficiency Syndrome / Acquired Immune Deficiency Syndrome) [1]. The causative agent for this disease is the human immunodeficiency virus. The yearly AIDS-related mortality has declined for the past 5 years due to the availability of highly active anti-retroviral therapy (HAART). Before HAART was available, a diagnosis of HIV-1 resulted in death in approximately 12 years from diagnosis [2]. In the United States, HAART has extended the lives of HIV patients by an estimated 30 years, transforming HIV/AIDS into a chronic condition [3]. This switch from fatal disease to chronic infection has led to development of anti-retrovirals that emphasize decreased toxicity and side effects [4].

Five major classes of antiretroviral therapy are currently prescribed, including entry inhibitors and specific inhibitors of three HIV proteins (Table 1). Generally, HAART is administered as combination therapy consisting of two nucleoside reverse transcriptase inhibitors and either a protease inhibitor or a non-nucleoside reverse transcriptase inhibitor [5]. Unfortunately, these therapies frequently lead to side effects, including cardiovascular disease, neurocognitive impairment, hepatotoxicity, and changes in lipid metabolism and fat deposition [6]. These can be

so severe that "structured treatment interruptions" have been used in an attempt to alleviate toxicity [7].

Table 1: Current classes of antiretroviral drugs.

Class	Target	Inhibition	Mechanism
Nucleoside RT inhibitors	Reverse Transcriptase	Competitive	Chain termination of new DNA strand
Non-Nucleoside RT inhibitors		Non-competitive	Inactivation of RT enzyme
Protease inhibitors	Protease	Competitive	Block generation of mature proteins
Integrase inhibitors	Integrase	Non-competitive	Block strand transfer
Entry inhibitors	Co-receptor	Competitive	Prevent binding of virus to uninfected cell
	Fusion	Non-competitive	Prevent virus from crossing cell membrane

Treatment interruption poses serious risks to the overall success of HAART. The high mutation rate of the HIV-1 virus fosters the development of drug-resistant strains. Rigorous adherence to therapy is necessary to control viral infection; missing a single day over the course of a month increases the risk of treatment failure six-fold [8]. Even with strict adherence to the drug regimen, 5% of patients on HAART develop drug resistance within the first year of therapy [9]. Treatment interruptions have been discontinued as a therapeutic option due to the increased risk of developing drug resistant viral strains.

Current antiretroviral therapy provides a treatment, not a cure, for HIV/AIDS. Even in the absence of treatment failure, viral reservoirs such as macrophages and resting T cells prevent total viral clearance even during an extensive HAART regimen [10-12]. The development of drug-resistant viral strains leads contributes to treatment failure of individual drugs and/or entire drug classes [13]. New members of existing drug classes are sought that minimize the harmful

side effects of long-term antiretroviral therapy and that provide alternatives that restore drug activity in the face of drug resistant HIV-1 strains [14-16]. In addition to new members of existing anti-retroviral drug classes, investigators have begun to develop therapies against additional viral proteins and interactions between the virus and the host cell [17-23]. These novel targets could provide more options for salvage therapy after HAART failure and improve the overall efficacy of HIV therapy.

2.0 BACKGROUND

2.1 HUMAN IMMUNODEFICIENCY VIRUS

The human immunodeficiency virus type 1 (HIV-1) is a member of the *Retroviridae* family belonging to the genus *Lentiviridae*. It is an enveloped virus containing two copies of its single-stranded RNA genome. Like most members of the retrovirus family, it uses *gag*, *pol*, and *env* genes to encode its structural and enzymatic proteins. HIV-1 also encodes two regulatory proteins (Tat and Rev), and four accessory proteins (Vif, Vpr, Vpu, and Nef) (Figure 1).

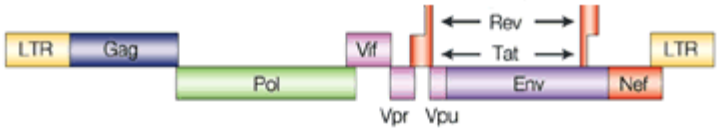

Figure 1: The HIV genome. The HIV genome includes both structural and accessory genes and is flanked on both ends by the HIV-1 LTR (long terminal repeat) promoter region.

The structural and regulatory proteins of HIV-1 each have a single function in the HIV life cycle [24]. The structural genes *gag*, *pol* and *env* encode polyproteins with multiple subunits. The Gag polyprotein is composed of matrix, capsid and nucleocapsid, the structural proteins of the virion. *Env* encodes gp120 and gp41 proteins, which are displayed on the surface of the virion to facilitate binding and entry. *Pol* encodes the enzymes of HIV-1: reverse transcriptase, integrase, and protease. The regulatory protein Tat is necessary for viral gene transcription, and Rev is involved in the export of viral RNA from the nucleus to the cytoplasm for translation. The

accessory proteins of HIV-1 are multifunctional and modify the individual cell environment to ensure viral replication, release and transmission [25] (Table 2).

Table 2: Role of HIV-1 Accessory Proteins in Viral Pathogenesis.

Function	Protein	Cellular Target
Infection of Specific Cell Types	Vpr	Macrophages, resting T cells
Inhibition of Cytoplasmic Defenses	Vif	APOBEC3 RNA editing
Modulation of Antiviral Activities at the Cell Surface	Vpu	Tetherin
Proteasome-mediated Degradation	Vif, Vpu, Vpr	Cullin ubiquitin ligases
Down-modulation of Host Cell Surface Molecules	Nef	CD4, T cell receptor, MHC class I
	Vpu	CD4
Modulation of the Intracellular Environment	Vpr	Cell cycle arrest, Apoptosis, Transcriptional regulation

The life cycle of HIV-1 is divided into distinct stages (Figure 2). The virus binds to cell surface molecules and fuses with the host cell membrane. In the cytoplasm, uncoating of the viral RNA occurs, and the viral RNA is reverse transcribed into DNA.

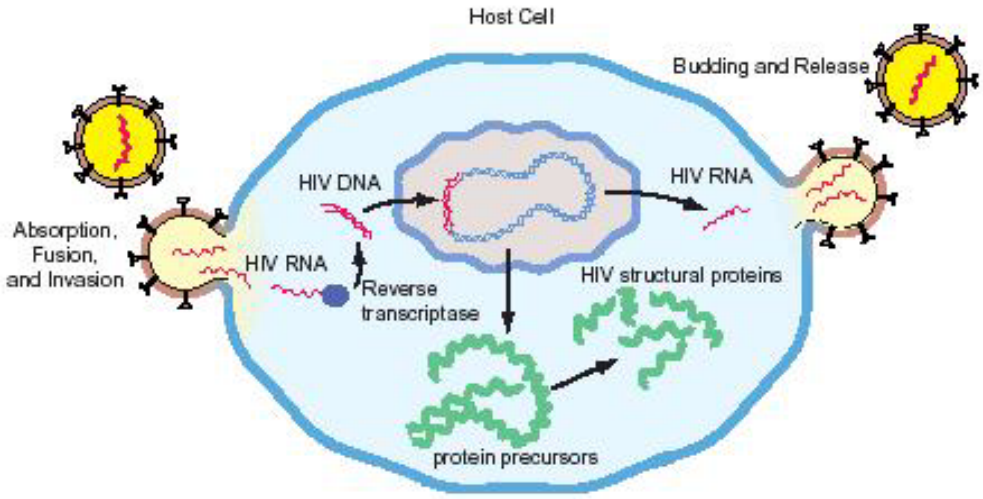

Figure 2: The replication cycle of HIV-1. HIV-1 enters the cell and reverse transcription occurs in the cytoplasm. Viral DNA integrates with cellular DNA, leading to the production of viral proteins which assemble at the cellular membrane. The virus matures and is released into the extracellular environment.

The pre-integration complex (PIC) forms and enters the nucleus of the cell. Viral DNA is integrated into the host cell's DNA, and transcription of viral RNAs occurs. Viral RNAs are translated, processed into individual proteins, and assembled in the cytoplasm. At the plasma membrane, the viral particle matures and is released into the extracellular environment.

HIV-1 infects cells of the immune system, simultaneously hampering a cell's ability to effectively combat the infection and taking advantage of the immune synapse to spread to adjacent cells. The initial target cells of HIV-1 infection include macrophages, dendritic cells, and CD4+ T lymphocytes [26].

2.2 DRUG TARGETS IN HIV INFECTION

2.2.1 Approved Therapeutics

In 1987, the reverse transcriptase inhibitor AZT was approved as the first therapy for HIV/AIDS [27]. This drug, and others that have followed it, is a nucleoside-analog reverse transcriptase inhibitor (NRTI). NRTIs compete with regular nucleotides for incorporation into the nascent DNA strand during reverse transcription and prevent the production of full-length viral DNA [28]. There is another class of reverse transcriptase inhibitors on the market: non-nucleoside reverse transcriptase inhibitors (NNRTIs). NNRTIs bind directly to reverse transcriptase and cause a conformational change in the enzyme that disrupts the active site and prevents it from synthesizing new viral DNA [29].

The first protease inhibitor was approved in 1995. Protease inhibitors prevent the cleavage of viral polyproteins into individual proteins and enzymes. Most of the inhibitors on the market are competitive inhibitors that mimic the shape of the natural substrate of protease [30]. Widespread resistance to current protease inhibitors has been seen in patients, and resistance mutations have been identified in both the protease enzyme and in the Gag polyprotein substrate [31].

The first integrase (IN) inhibitor was approved in 2007, and it remains the only IN inhibitor on the market. It inhibits the strand transfer function of integrase by binding to the enzyme-DNA complex and trapping it in an intermediate state so that the proviral DNA cannot be inserted into the host cell genome [32].

At the cell surface, therapeutics are available that target HIV-1 entry and fusion. Fusion inhibitors target the tethering of viral envelope to host cell membrane by gp41. There are multiple targets in the entry process, including CD4, CXCR4 and CCR5. Of these targets, only one has made it to market: a co-receptor antagonist to the chemokine receptor CCR5. Antagonists to the CXCR4 receptor are in clinical trials, as are monoclonal antibodies against the CD4 receptor [33].

2.2.2 Novel Work on Existing Drug Classes

Additional inhibitors of reverse transcriptase (RT) have been identified *in vitro* and one has reached the clinical trial phase. KP-1212 uses the high mutation rate of the HIV genome against itself. It is a nucleoside that does not induce chain termination but rather induces viral mutagenesis with the goal of crossing the threshold for error capacity and ablating the viral

population as a whole [34]. Other groups have focused on inhibiting the RNaseH domain of RT or destabilizing the dimer needed to form the active RT enzyme [35, 36].

Novel strategies for targeting the protease enzyme include non-competitive inhibitors that bind to the flap of the enzyme, competitive inhibitors that fit closely within the substrate envelope region of protease, or small molecules that disrupt the dimerization of the enzyme [37-39]. Novel strategies for targeting the integrase enzyme include targeting the viral DNA binding step, inhibiting interaction with the cellular chromatin-tethering protein LEDGF, disrupting the dimerization and/or tetramerization properties of integrase, and disrupting the interaction with the viral cofactor Rev [40-43]. Novel strategies that target entry include the inhibition of gp160 cleavage in infected cells [44].

2.2.3 Novel Targets

Novel targets for antiretroviral therapies are being sought throughout the viral life cycle (Table 3). Inhibitors of the late stages of viral replication (assembly, maturation and release) have generated particular interest, and the maturation inhibitor bevirimat has entered clinical trials [45, 46]. Inhibitors of regulatory proteins and accessory proteins are also the subject of significant research. In addition to the targets in Table 3, which all have an effect on a single stage in the viral life cycle, inhibitors that target complex interactions in the host cell are also under development. The interaction of the accessory protein Nef with cellular kinase Hck has been found to be necessary for productive viral replication and thus is under scrutiny [47]. Vpr-mediated apoptosis and cell cycle arrest have also been targeted [48, 49].

Table 3: Novel Molecular Targets for Antiretroviral Therapy.

Viral Protein	Viral Replication Step	Molecular Target/Mechanism	Reference
Tat	Transcription	Tat-TAR interaction	[50]
Rev	Translation	Rev nuclear export	[51]
Gag	Release	Gag-TSG101 interaction	[52]
Gag	Maturation	Gag processing cascade	[46]
Capsid	Assembly	Capsid oligomerization	[53]
Nucleocapsid	Assembly Reverse Transcription	Ejection of catalytic zinc molecule	[54]
Vpu	Release	Vpu-tetherin interaction	[55]
Vif	Reverse Transcription	Vif-APOBEC interaction	[56]

Other HIV-1 targeting strategies focus on more global targets. Latent reservoirs are a source of considerable interest because they prevent anti-retroviral therapy from curing patients of the disease. The main latent reservoir of HIV-1 is thought to be resting CD4+ T cells. Agents aimed at both non-specific and selective activation of HIV-infected CD4+ T cells have been identified [57, 58]. Other therapeutic strategies, known as virostatics, are aimed at reducing the level of chronic immune activation [21].

The avenues that are being explored for HIV-1 therapeutics have widened considerably beyond the enzyme and cell surface molecules based treatments currently available. In particular, protein-protein interactions and dimerization have become feasible drug targets. With this new line of research has come a wave of research in therapies targeted at regulatory and accessory proteins.

2.3 PROTEIN-PROTEIN INTERACTIONS

Protein-protein interactions (PPI) play critical roles in most cellular processes. Signal transduction cascades, membrane-bound receptor signaling, and ion channel formation are mediated by protein-protein interactions, and at its most basic level the antigen-antibody interaction is also considered a type of PPI [59]. Many viral proteins and enzymes require dimerization to become active, and the case of HIV-1 is no exception. Reverse transcriptase is a heterodimer, and protease is a homodimer composed of two identical subunits [36, 39]. The active site of integrase is present at the dimerization interface, and it is present as a dimer in the cytoplasm and a tetramer in the nucleus [42]. Similarly, HIV-1 Tat, Rev, Vif, Nef, and Vpr have also been found to dimerize *in vivo* [60-64].

2.3.1 Structural Features

Protein-protein interactions share several key structural features that can be used to determine their likely binding sites. Most protein interfaces are a result of higher level structural organization of a protein, not the sequence of its amino acids [59]. As a result, knowing a protein's molecular and/or crystal structure is often necessary for drug development. A potential dimer interface can be identified as a hydrophobic patch on the surface of a protein [65]. Protein interfaces, once thought to be large and flat, are actually composed of binding hot spots that involve relatively few amino acids [66].

Knowing these hot spots can aid in rational and structure-based design of inhibitors (Figure 3). The rest of the interface is composed of anchor residues and residues with high flexibility to

accommodate the binding of ligands [67]. The knowledge of the structure of a protein and its interaction partner is beneficial in drug development.

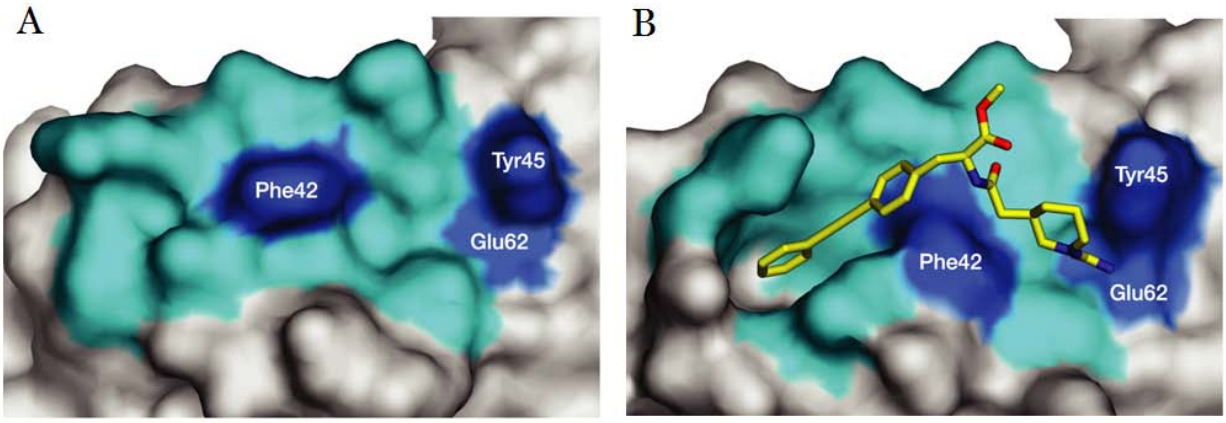

Figure 3: Example hot spot distribution on a protein-protein interface. The protein interface of the IL-2 interleukin receptor is shown (A) in the absence of ligand and (B) bound to IL-2. Hot spot resides are shown in dark blue and adjacent interface residues are shown in light blue. Modified from [65].

2.3.2 Methods to Detect Dimerization

Without an easily measured endpoint like that of an enzyme, protein-protein interactions had been ignored by the drug development community. The emergence of assays that detect interactions has changed that. Bait and prey methodologies such as the yeast two-hybrid system are a useful tool to ascertain the binding ability of two proteins; however, the yeast two hybrid system was limited in its ability to detect certain types of PPI. Advances have been made to allow not only the screening of cytoplasmic and membrane-bound proteins, but also to develop a mammalian two hybrid equivalent [68]. Additional advances in bait and prey systems have resulted in a variety of protein complementation systems, in which a molecule is split into two pieces and regains its functionality when the molecules are brought into close proximity by protein-protein interaction or dimerization [69].

Fluorescence-based systems are a common detection system for dimerization due to the close proximity of the two proteins. Dimerization can be detected as either a quenching or release of fluorescence, depending on the bait and prey combinations. For cell-based assays, flow cytometry or automated fluorescence microscopy is used to measure a change in fluorescence intensity. FRET-based assays use a dual fluorophore system in which the emission of fluorescence from the first molecule excites the second, and the intensity of the fluorescence at the second emission wavelength is measured [70]. High throughput screening uses soluble proteins *in vitro* to assess binding through changes in fluorescence [71].

2.3.3 Targeting Dimerization

Many strategies have been used to design molecules that target protein-protein interactions. Structure-based and rational design use co-crystallization of multiple ligands and/or fragments of known interacting proteins to determine the structure of the interface when a molecule is bound and creates a pharmacophore that shows ideal points of contact [41]. The consensus pharmacophore is used to electronically screen for small molecules that match these points of contact, and the results of this search are tested experimentally [72]. In fragment-based design, the initial hits are normally weak and techniques to increase the binding affinity of a fragment hit have been developed [73].

There are ways to improve the strength of PPI inhibitors beyond the synthesis of structural analogs. A fragment with weak or moderate binding affinity can benefit from the addition of a group with weak chemical reactivity designed to create a covalent bond with the protein target. The formation of covalent bonds is, as a general rule, avoided in drug development due to the

potential for non-specific interactions; however, the use of a weakly reactive group decreases the likelihood of these non-specific interactions [74]. This has been used to great effect in the treatment of prostate hyperplasia with the small molecule finasteride [75].

2.4 THE VIRAL PROTEIN R (VPR)

The accessory protein Vpr is a multifunctional protein that plays a role in many aspects of HIV-1 pathogenesis. Vpr arrests the cell cycle at the G2/M phase and induces apoptosis in bystander cells [76, 77]. It is also involved in immune suppression and neuropathogenesis [78-81]. Vpr is packaged into the virion, and it plays a role in the early stages of infection through transactivation of viral transcription and transport of the pre-integration complex into the nucleus [82-86]. Vpr has also been shown to facilitate the infection of macrophages and non-dividing cells [87, 88].

2.4.1 Vpr Structure

Vpr is a protein composed of 96 amino acids with a molecular weight of approximately 14kDa. It has three alpha helices that form a hydrophobic core. Vpr associates into dimers, trimers and higher order oligomers in a concentration-dependent manner, and all three helices have been implicated in oligomerization [82, 89-91].

Deficiencies in dimerization have been shown to affect cellular localization and to prevent incorporation into the viral particle [82, 92]. Vpr-deficient virus particles are less effective at

infecting macrophages, which are one of the primary targets of HIV-1 infection [93]. Without incorporation into the viral particle, Vpr cannot assist in early infection through transactivation of the LTR, nuclear import of the pre-integration complex, or modulation of the viral mutation rate via association of Ung2 [88]. Intentional inhibition of Vpr dimerization may have therapeutic benefits.

No crystal structure of Vpr is available due to the formation of insoluble protein aggregates at the concentrations required to crystallize proteins; however NMR data has been obtained for the full length protein in two different solvents [90]. Our laboratory has used this NMR data to generate models of the dimerized form of Vpr (Figure 4).

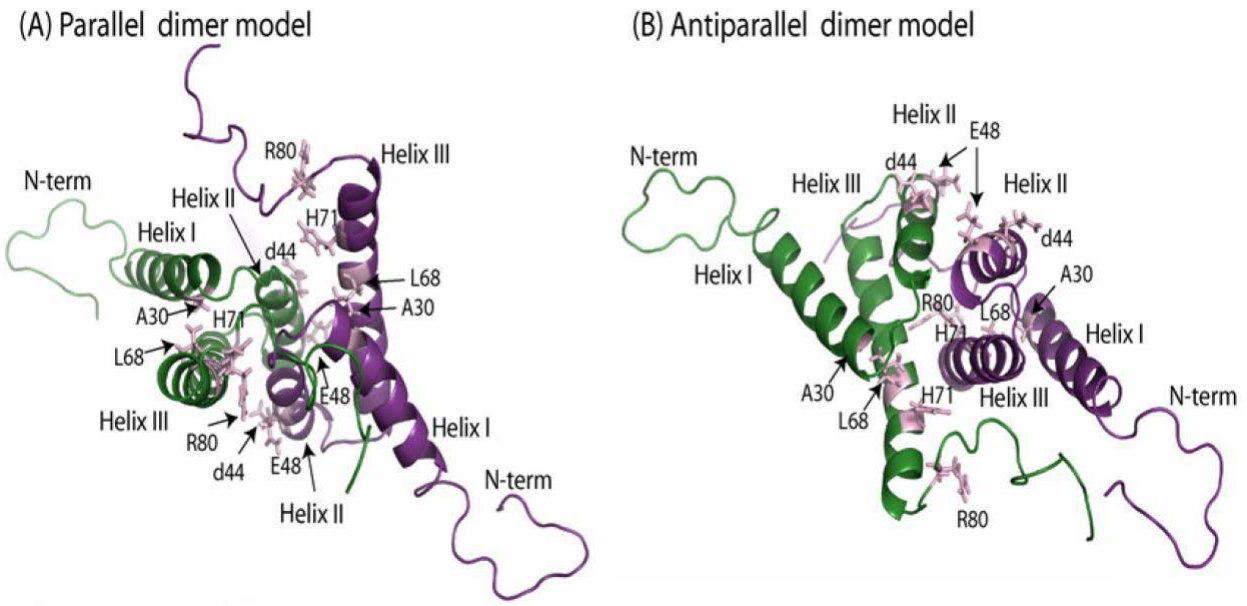

Figure 4: Proposed dimer orientations for Vpr. Two possible configurations for the dimerization of Vpr were generated from full length NMR structures using computational modeling. (A) Proposed parallel configuration of the dimer. (B) Proposed antiparallel configuration. [82]

Mutagenesis studies have shown that over 10 point mutations can result in dimerization deficient Vpr [91]. These mutations are spread over all three helices, but the majority are thought to be

involved in the stability of the hydrophobic core and not available for a protein-protein interface. The residues positioned to allow for inter-molecular interactions are Q44 from helix 2, and L67 from helix 3.

2.4.2 Known Inhibitors of Vpr

HIV-1 Vpr is a multifunctional protein. Several groups have discovered inhibitors of selected Vpr functions. The majority of the studies focused on inhibition of Vpr-mediated cell death and growth inhibition due to cell cycle arrest. Eight inhibitors have been found, and they are summarized in Table 4.

Table 4: Known Inhibitors of Vpr Functions

Inhibitor	Discovery Method	Functions Inhibited	Reference
Pentoxifylline	Yeast screen	Cell cycle arrest, apoptosis	[94]
Hexameric peptides with di-tryptophan motif	Yeast screen	Cell cycle arrest, apoptosis	[95]
Fumagillin	Yeast screen	Cell cycle arrest, apoptosis	[49]
Damnacanthal	VLP-infection	Apoptosis	[48]
Mifepristone	Co-transfection	LTR transactivation	[96]
Hematoxylin	In-vitro binding	Nuclear transport of PIC through importin-alpha	[17]
SIP-1	In-vitro binding	Macrophage infection	[97]
Vipirinin	Yeast screen	Cell cycle arrest	[98]

Screening for over half the published inhibitors occurred in yeast systems. The mammalian systems used transfection and transduction to introduce Vpr to cells in an effort to reduce cell death. Newer assays have incorporated protein arrays on slides or adsorbed to an ELISA plate. Three inhibitors have been found that inhibit multiple functions of Vpr. An apoptosis-specific inhibitor and a cell cycle arrest specific inhibitor have also been discovered. Less common

targets such as nuclear transport and transactivation have also been targeted; however, no screen has been undertaken to interfere with the oligomerization properties of Vpr.

Here, I propose to develop a cell-based screen to target HIV-1 protein oligomerization, using the oligomerization of Vpr as a "proof-of-concept". After optimizing and validating this screening system, I will apply it to two libraries with the goal of identifying a compound that inhibits the dimerization properties of Vpr. Whether the libraries yield an inhibitor or not, the validation of this screen for oligomerization is easily adaptable to additional dimeric protein and can have a wide range of use in the study and screening of protein-protein interactions.

3.0 THESIS AIMS

The success of HAART has turned HIV-1 infection into a chronic disease. However, existing antiretroviral therapies have serious side effects, and viral escape mutants can develop against entire classes of HIV drugs. The necessity of developing new antiviral compounds to treat HIV-1 infection has led to the investigation of virus-encoded proteins including the accessory protein Vpr, which has multiple functions in HIV-1 pathogenesis.

Macrophages are an important target for HIV-1, both in initial infection and as reservoirs of virus. The infection of macrophages requires the incorporation of Vpr into the viral particle so that it may assist with translocation of the pre-integration complex into the nucleus. Vpr-deficient virions have been shown to produce a less robust infection of macrophages. It has been determined that one of the mechanisms needed for Vpr incorporation into the viral particle is Vpr-Vpr oligomerization. In the absence of oligomerization, Vpr molecules are unable to interact with Gag and be packaged into virions.

The three major aims of this thesis included first characterizing a fluorescence complementation system for detection of oligomerization. Secondly, we wanted to determine whether the sensitivity existed to make quantitative assessments about oligomerization. Thirdly, we wanted to view the effect of two small libraries on Vpr-Vpr oligomerization.

AIM #1: To characterize the bimolecular fluorescence complementation system for detection of oligomerization

A) To develop a reproducible co-transfection system for bimolecular fluorescence complementation (BiFC).
B) To determine localization of the BiFC signal.
C) To determine kinetics of protein expression and BiFC detection.
D) To assess the level of non-specific BiFC signal.

AIM #2: To quantify a decrease in fluorescence using a competition assay

A) To develop a competition assay using untagged Vpr.
B) To quantify fluorescence through flow cytometry.
C) To quantify fluorescence through immunofluorescence.

AIM #3: To assess libraries for an effect on Vpr oligomerization

A) To determine optimum concentrations of solvent and libraries.
B) To validate a high content imaging screen.
C) To assess a library of Vpr peptides.
D) To assess a library of small molecule leucine rotamers.

4.0 MATERIALS AND METHODS

4.1 CELL LINES

HeLa and HEK293T cell lines were grown in DMEM (Gibco) supplemented with 10% FBS (HyClone), 1% Penicillin-Streptomycin (Invitrogen), and 1% L-glutamine (Invitrogen) [D-10]. HeLa and HEK293T cells were grown in 5% CO_2 at 37°C. HeLa cells were obtained through the NIH AIDS Research and Reference Reagent Program, Division of AIDS, NIAID, contributed by Dr. Richard Axel. HEK293T cells were given by Dr. Michelle Calos, Stanford University, CA.

4.2 PLASMIDS

All plasmids were generated by propagation in DH5alpha bacterial cells, and DNA was extracted using the Qiagen MaxiPrep kit (QIAGEN). Mammalian expression plasmids for HIV-1 Vpr containing either an HA-tag at the N-terminus or a Flag-tag at the C-terminus were used as "untagged" Vpr in the competition assays.

The Venus N and Venus C fusion constructs used in this paper were generated by Dr. Jay Venkatachari as described in [82]. Briefly, sequences encoding the amino (residues 1-173; VN) or carboxyl (residues 155-238; VC) fragments of Venus fluorescence protein were fused to the N

terminus of HIV-1 Vpr via a six alanine linker sequence and an HA-tag for detection (Figure 5). Venus constructs of wildtype Vpr, Q44, and A30L were used.

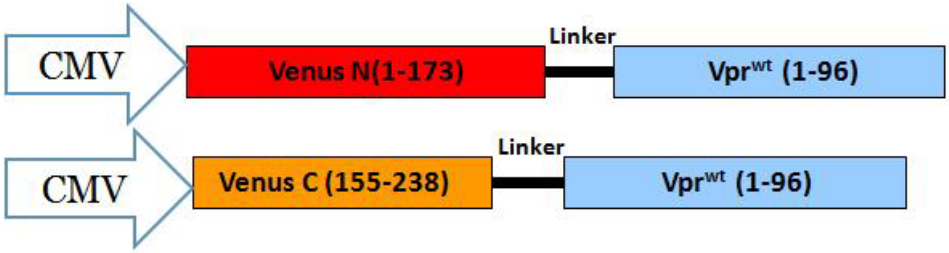

Figure 5: Venus plasmid constructs.

4.3 TRANSFECTION METHODS

4.3.1 Calcium Phosphate

The calcium phosphate method was used on HEK293T and HeLa cell lines. Cells were plated to reach 70% confluence. Three hours prior to cell transfection, cell media was replaced with fresh D-10 media. The transfection was conducted by adding DNA (450µL) to water (450µL) to 2.5M $CaCl_2$ (50µL). To the DNA-water-$CaCl_2$ mix, 50mM BES (BES, 250mM NaCl, 0.5mM Na_2HPO_4) (500µL) was added and the mixture was incubated at room temperature for 30 minutes. After incubation, the mixture was added dropwise to cells. Within 6-12 hours, the media on the cells was removed, the cells were washed once with PBS to remove all precipitate and excess DNA, and fresh D-10 was added.

4.3.2 Lipofectamine Transfection

Lipofectamine 2000 transfection was used on HeLa cells according to manufacturer's protocol. Briefly, cells were plated and grown to 70% confluence. 30 minutes prior to transfection, cells were given fresh D-10 media. Plasmid DNA was mixed with DMEM and Lipofectamine 2000 (Invitrogen). The DNA-Lipofectamine complex was incubated at room temperature for 20 minutes then added dropwise to cells. After 5 hours, media was removed, cells were washed to remove any excess DNA or Lipofectamine, and fresh D-10 media was added.

4.3.3 PolyJet Transfection

PolyJet transfection was used on HEK293T and HeLa cells according to manufacturer's protocol. Briefly, cells were plated and grown to 75% confluence. 30 minutes prior to transfection, cell media was replaced with fresh D-10 media. The transfection was conducted by diluting plasmid DNA in DMEM, then adding PolyJet DNA Transfection Reagent (SignaGen) diluted in DMEM. The DNA-PolyJet complex was incubated for 15 minutes then added dropwise to cells. After 5-24 hours, the DNA-PolyJet complex was removed and fresh D-10 media was added.

4.4 SMALL MOLECULE LIBRARIES

4.4.1 Vpr Peptide Library

A library of HIV-1 Consensus B VPR (15-mer) Peptides was obtained from the NIH AIDS Research and Reference Reagent Program, Division of AIDS, NIAID, NIH. The library contains 22 peptides, 15 amino acids in length, with 11 amino acid overlaps between sequential peptides. Peptides were reconstituted from lyophilized powder in solvents (H2O, PBS, or DMSO) according to the NIH-provided solubility table (Appendix 1).

4.4.2 Leucine-based Small Molecule Library

A library of 45 leucine rotamers was a generous gift from Dr. Alexander Dömling (University of Pittsburgh). The library was received as 10mM stocks dissolved in DMSO.

4.5 IMMUNOFLUORESCENCE ANALYSIS AND IMAGING

The antibodies used for immunofluorescence experiments are monoclonal anti-HA (Sigma; 1:200) and monoclonal anti-Flag M2 (Sigma; 1:300). Transfected HeLa cells were grown on coverslips and fixed with 2% paraformaldehyde in PBS for 15 minutes. Coverslips were washed with PBS, treated with 0.1% Triton X-100 (Fisher Scientific) in PBS for 15 minutes, and washed again with PBS. Coverslips were blocked with PBS containing 2% bovine serum albumin (BSA; Sigma) for 45 minutes and incubated for 90 minutes at 37°C with primary antibodies as

described above, followed by additional washing with 0.5% BSA in PBS. Coverslips were incubated with Cy5-tagged secondary antibody (Jackson ImmunoResearch; 1:800) for 60 minutes then washed with 0.5% BSA in PBS. Hoechst 33342 nuclear stain (Sigma) was applied for 2 minutes and coverslips were washed with PBS. Gelvatol mounting media was provided by the Center for Biological Imaging (CBI) to adhere coverslips to slides.

Confocal multicolor images using the FITC, Cy5 and DAPI channels were recorded using an Olympus Fluoview 500 upright microscope at the Center for Biologic Imaging at the University of Pittsburgh School of Medicine. Spot intensity quantitation was performed using MetaMorph II software at the Center for Biologic Imaging. The images were thresholded to reduce background noise, and the nuclear region was selected in the FITC channel of an image. Region statistics were used to record the average intensity of the FITC signal in the nucleus and its standard deviation.

4.6 WESTERN BLOT

Cells were lysed using lysis buffer containing 50mM Tris (pH 7.5), 150mM NaCl, 1% Triton X-100, 1mM sodium orthovanadate, 10mM sodium fluoride, 1.0mM phenylmethylsulfonyl fluoride, 0.05% deoxycholate, 10% sodium dodecyl sulfate, aprotinin (0.07 trypsin inhibitor unit/ml), and the protease inhibitors leupeptin, chymostatin, and pepstatin (1μg/ml; Sigma) and protein levels were quantitated with the Pierce BCA Protein Assay kit (Thermo Scientific). Protein (30μg) was run on a 12% SDS-PAGE gel. Proteins were transferred to Immobilon PVDF membrane (Millipore) and the membrane was blocked in 2% BSA for 1 hour. Membranes were

incubated in primary antibody overnight at 4°C and washed in PBS containing 0.1% Tween-20 (PBS-T; Fisher Scientific). Secondary antibody was applied for one hour at room temperature. Membranes were exposed to Pierce SuperSignal West Pico chemiluminescent substrate (Thermo Scientific) then developed.

4.7 FLOW CYTOMETRY

Twenty hours post-transfection, HeLa cells were trypsinized and pelleted. Cells were fixed in 4% paraformaldehyde for 10 minutes, then pelleted and resuspended in 5% fetal bovine serum in PBS. Data was collected using a BD FACSCanto flow cytometer (Becton Dickenson) and FACSDiva software (Becton Dickenson). Cells were gated according to the following parameters. Forward and side scatter were used to identify the live population, and 20,000 live events were recorded. The FITC positive gate was set based on cells "mock" transfected with empty pcDNA 3.1 vector. The gate was positioned to contain no more than 1% of mock-transfected cells. The mean fluorescence intensity was obtained from this gate. Data was analyzed using Flow Jo software.

4.8 COMPETITION ASSAYS

Cells were grown to 75% confluence in 6 well plates. Cells were transfected with a total of 2µg of plasmid DNA according to PolyJet protocol. Equal amounts of VN-Vpr^{wt} and VC-Vpr^{wt} were added to each well, and the total quantity of VN- and VC- Vpr was referred to as "Venus Vpr."

Ratios were created to represent the amount of Venus-Vpr to untagged Vpr in each transfection. The ratios ranged from 1:0 to 1:10. A negative control of 0:1 was used, containing the same quantity (in ng) of untagged Vpr as the quantity of Venus-Vpr in the corresponding 1:0 control. Twenty hours post-transfection, cells were collected for Western blot and flow cytometry analysis.

4.9 SCREENING ASSAYS

Cells were grown to 75% confluence in a $10cm^2$ plate and transfected with equal quantities of VN-Vpr and VC-Vpr. Five hours post-transfection, cells were washed with PBS, trypsinized, and replated into a 96 well plate at a density of 9,000 cells/well in 200µL of D-10. Wells were treated in triplicate with 2µL of a compound. Plates were incubated at 37°C for a total of 24 hours post-transfection.

4.9.1 Cytotoxicity

To determine the percentage of cellular toxicity in vitro of each compound, the MTT Tetrazolium assay was performed. Twenty-four hours post-transfection, 20µL of 5mg/mL thiazolyl blue tetrazolium bromide (Sigma) was added to each well. Four hours later, cell media was removed and replaced with 100µL DMSO (Sigma).

4.9.2 Flow cytometry

Twenty-four hours post-transfection, cells were washed and trypsinized in the 96 well plate. Cells were spun down, resuspended in 4% paraformaldehyde for 15 minutes. Cells were spun down and resuspended in 5% FBS in PBS. The plate was run using the plate reader functionality of a BD LSRII flow cytometer (Becton Dickenson). Data was analyzed using Flow Jo software.

4.9.3 High Content Imaging

Cells were washed twice with PBS and fixed with 4% paraformaldehyde for 15 minutes. Cells were washed in PBS and stained with Hoechst nuclear stain (Sigma) for 1 minute. Cells were stored in 100µL PBS, and plates were sealed with MicroAmp sealing film (Applied Biosystems).

Plates were analyzed by automated fluorescence microscopy using the ArrayScan V^{TI} HCS Reader imaging cytometer (Thermo Scientific Cellomics). Data was collected in the FITC, TRITC and DAPI channels. Data was analyzed using the BioApplications platform (Thermo Scientific). Background fluorescence was eliminated through comparison of FITC and TRITC channel intensities. Using this filtered set, cells with a small nuclear area were excluded to eliminate the dead/dying population. The remaining cells were analyzed for mean nuclear FITC intensity. Data collection and analysis was performed by the Cytometry facility at the University of Pittsburgh Cancer Institute with assistance from William Buchser.

5.0 RESULTS

5.1 AIM #1: TO CHARACTERIZE THE BIMOLECULAR FLUORESCENCE COMPLEMENTATION SYSTEM FOR DETECTION OF OLIGOMERIZATION

5.1.1 Bimolecular Fluorescence Complementation

To detect Vpr-Vpr dimerization/oligomerization, we have utilized a variation on the bait and prey system known as protein fragment complementation. Protein fragment complementation uses two fragments of a single protein that is reconstituted through the interaction of its two halves [99]. Many protein fragment complementation systems exist, such as those for ubiquitin, dihydrofolate reductase, and split luciferase [100-102]. Bimolecular fluorescence complementation (BiFC) uses a split fluorescent protein fused to the protein(s) of interest to detect their interaction (Figure 6).

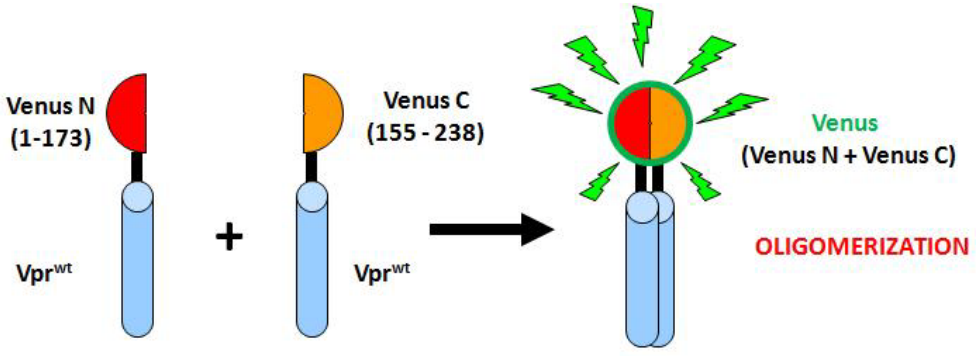

Figure 6: Schematic representation of BiFC system. Restoration of fluorescence occurs through oligomerization of fusion proteins.

We are using the YFP-derived Venus fluorophore, which is divided into an N terminal (amino acids 1-173) and C terminal fragment (amino acids 155-238). For simplicity, these fragments will be referred to as VN and VC for the duration of this paper.

5.1.2 BiFC Assay Parameters

From the start of assay development, the ultimate goal was to design a high content screen that would be read in a 96 well plate. Two possible transfection strategies were considered: seeding cells directly into a 96 well plate and transfecting each well individually, or seeding cells into a larger plate for transfection then moving them to a 96 well plate. We chose the latter because performing 96 individual transfections would introduce added well-to-well variability in transfection efficiency that could skew the interpretation of results. One disadvantage of this method is the need to replate the cells because trypsinization is stressful for cells. This was taken into account when choosing a cell line; each line was tested under these experimental conditions to determine whether it could handle the added stress of replating.

BiFC is a fluorescence reporter assay which is used both quantitatively via flow cytometry and qualitatively via immunofluorescence microscopy [69]. Smaller, suspension cells are preferred for flow cytometry, and larger cells are more suited for image-based analysis. Though the final form of the assay is a high content screen, preliminary work was performed using flow cytometry. Adherent cells that are screened with flow cytometry must be able to survive trypsinization three times in 48 hours, so the cell line needed to be hardy and the transfection agent needed to be non-cytotoxic.

5.1.2.1 Selection of Cell Line

We began with HEK293T cells due to their capacity for high protein expression, but HEK293T cells are not ideal for the multiple washes necessary in preparation for flow cytometry. Despite efforts to wash cells gently, greater than 40% of cells were lost in the preparation process. Of the cells that remained, only 20-30% were positive for fluorescence. In addition to the cell loss, significant morphological changes in the forward and side scatter were observed between the non-transfected and transfected cells, most likely due to cellular stress from the replating (Figure 7). These factors eliminated HEK293T as a model cell line. We next tried the non-adherent Jurkat cell line but were unable to transfect the cells by calcium phosphate, Lipofectamine 2000, or nucleofection methods.

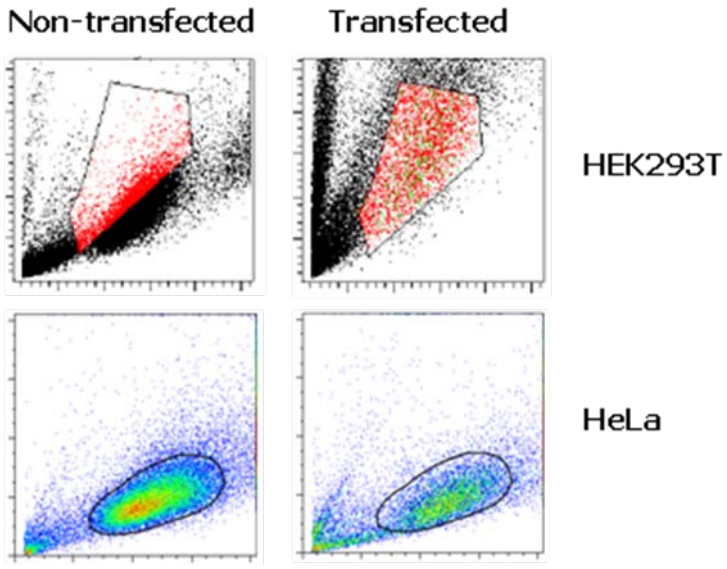

Figure 7: Morphological changes after transfection protocol. Transfected cells were replated 6 hours post-transfection and collected for flow cytometry analysis at 24 hours. Un-transfected cells were collected for flow directly from a culture flask

Our third choice for cell line was the HeLa cell line. This assay is ultimately designed to be an imaging-based screen, for which large adherent cells, like those of the HeLa or COS-7 lines, are

ideal. Since HeLa cells are more tightly adherent than HEK293T cells, they tolerate the washings in preparation for flow cytometry better. After the replating procedure, HeLa cells did not show morphological changes like those seen in HEK293T cells (Fig. 7). We tested two different HeLa cell lines (HeLa and HeLa $T4^+$) and chose from these based on their responses to transfection reagents.

5.1.2.2 Selection of Transfection Reagent

In order to choose the optimum transfection reagent for our cell lines, we looked for two qualities: high transfection efficiency and low cytotoxicity. We ranked low cytotoxicity as more important than high transfection efficiency due to the added stress our assay will create due to the replating step. HEK293T cells were transfected according to a calcium phosphate protocol, but this protocol is not used in our laboratory for HeLa cells. HeLa cells were transfected first using Lipofectamine. After a co-transfection of the BiFC plasmid set, this system transfected 15% of both HeLa and HeLa $T4^+$ cells. Cytotoxicity was measured as the percentage of rounded or floating cells. Forty percent of HeLa cells and 55% of HeLa $T4^+$ cells exhibited cytotoxicity (Figure 8).

PolyJet DNA transfection reagent was tested on both HeLa cell lines as well as in HEK293T cells. The PolyJet system produced greater than 50% fluorescence from co-transfection in all three cell lines. HeLa $T4^+$ cells showed the highest co-transfection efficiency at 65%, and HeLa cells were slightly lower at 60%. PolyJet-induced cytotoxicity was lower than that of the calcium phosphate and Lipofectamine systems in all cell lines tested. The cytotoxicity was 5% in the HeLa cell line and 15% in the HeLa $T4^+$ cell line.

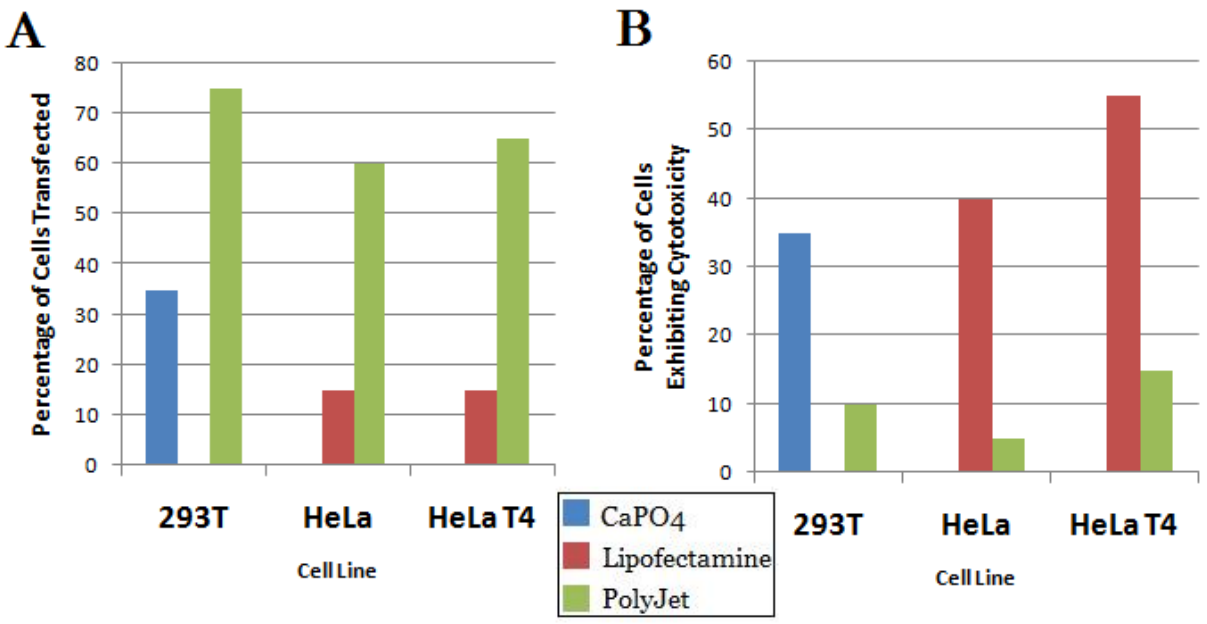

Figure 8: Efficiency and cytotoxicity of transfection in multiple cell lines. Cell lines were transfected according to calcium phosphate, lipofectamine or PolyJet protocol. 38 hours post-transfection, cells were observed under a fluorescence microscope for **(A)** percentage of fluorescent cells and **(B)** cytotoxicity as measured by morphological change and floating cells.

HEK293T cells were eliminated as a potential cell line due to toxicity from the transfection process, so cytotoxicity was seen as the most important criterion. Therefore, while HeLa $T4^{+}$ cells had higher transfection efficiency, its cytotoxicity led us to chose the HeLa cell line for the remainder of our experiments.

5.1.3 Localization of BiFC Signal

High content analysis is imaging-based, which gives it the capability to determine the localization of proteins. A nuclear stain is used to obtain a cell count, and the analysis software is capable of quantitating the nuclear and cytoplasmic fluorescence independently. In order to determine which analysis is more relevant to the Venus fragment-fused proteins, we looked at the localization of VN-Vpr and VC-Vpr in HeLa cells. Vpr is known to localize to the nuclear

membrane; however, larger fusions have been shown to exclude Vpr from the nucleus. Twenty - four hours post-transfection, cells were fixed and stained with antibody to the HA tag in the linker region in order to identify transfected cells (Figure 9).

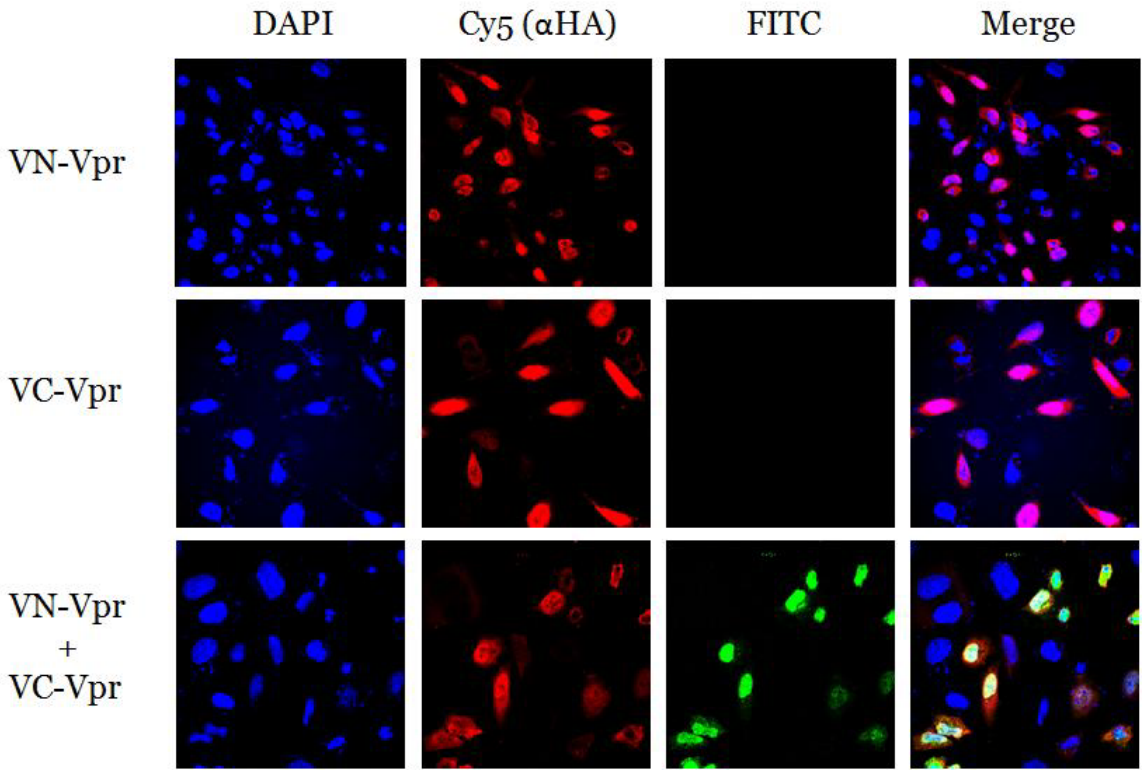

Figure 9: Localization of BiFC signal. Cells were grown on coverslips, transfected and fixed 24 hours post-transfection. Cells were stained with α-HA primary, Cy5-conjugated secondary and DAPI, and viewed under a confocal microscope at 60X magnification.

Both Vpr fusion proteins localize in and around the nucleus. VN-Vpr is found almost exclusively in the nucleus, whereas VC-Vpr has more diffuse localization throughout the cell. The transfections of VN- and VC- alone gave no BiFC signal in the FITC channel. The co-transfection exhibited robust BiFC signal that co-localizes with the HA staining. Since the BiFC signal is concentrated in the nucleus, we focused on the intensity of BiFC signal in the nucleus in the following aims 2 and 3.

5.1.4 Kinetics of Protein Expression

The reconstitution of the Venus fluorophore is irreversible. Therefore, in order to see an effect from an exogenously added peptide or small molecule, it is necessary to treat cells before the expressed proteins have a chance to interact. To determine when the fusion proteins are expressed in the cell, we co-transfected cells with equal amounts of VN-Vpr and VC-Vpr plasmid and collected cells at various times post-transfection.

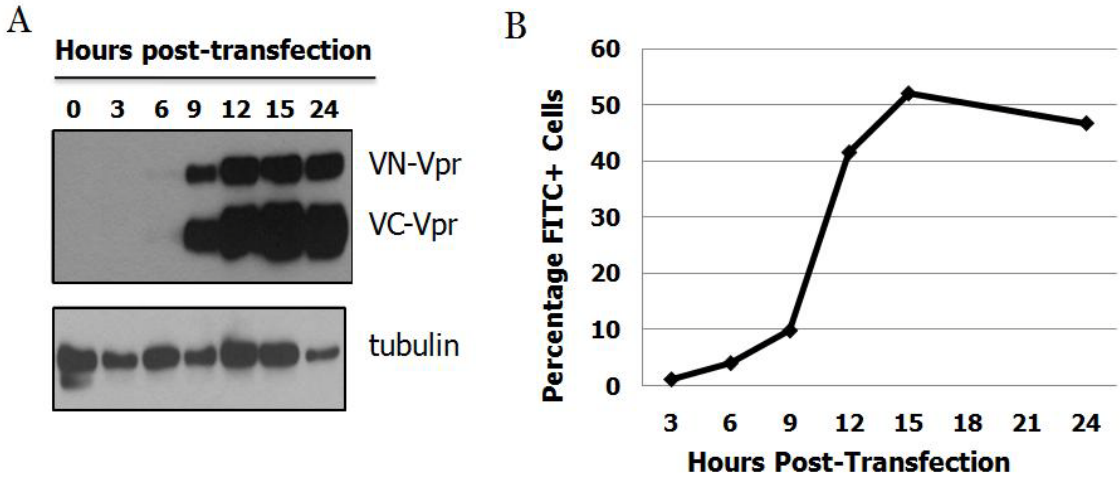

Figure 10: Protein expression in co-transfected HeLa cells. Cells were co-transfected with equal amounts VN-Vpr and VC-Vpr. At the indicated times post-transfection, cells were collected for further analysis. (A) Cells were lysed and analyzed via Western blot using anti-HA antibody. (B) Cells were fixed and analyzed with flow cytometry.

Protein expression can be detected as early as six hours post-transfection in HeLa cells, and by twelve hours the protein levels saturate the detection levels of the Western blot (Fig 11A). BiFC signal remains under 10% until twelve hours post-transfection (Fig 11B). The delay between protein expression and BiFC fluorescence detection is likely due to the maturation time needed for the reconstitution of the Venus molecule [103]. Since protein expression can be detected as early as six hours post-transfection, we determined that exogenous compounds should be added

to cells six hours post-transfection. In terms of assay set-up, we chose to trypsinize our cells and begin the replating process five hours post-transfection.

5.1.5 Specificity of the BiFC Interaction

Vpr-Vpr oligomerization occurs via random interaction between two Vpr molecules. In a transient transfection system, proteins are often overexpressed, increasing the likelihood of interaction inside the cell. The strong CMV promoters used in our Venus constructs are no exception. The restoration of the Venus fluorescent molecule occurs at distances under 100nm. Because of the increased protein levels in the cell and the tendency of Vpr to oligomerize, there is a risk of non-specific restoration of Venus fluorescence inherent in the BiFC system. To assess the frequency and strength of non-specific interaction, we used Venus plasmid sets with two Vpr mutants known to be dimerization deficient: Vpr^{A30L} and $Vpr^{Q\Delta44}$ [82]. We transfected cells with combinations of wildtype and mutant VN- and VC- Vpr and analyzed the percentage and intensity of cells that were positive by flow cytometry (Figure 11).

Forty-eight percent of the cells transfected with wildtype VN- and VC-Vpr were positive for BiFC signal. When the transfected VN- and VC- were both dimerization deficient, approximately 4% of cells were positive for BiFC signal. When transfected with wildtype VN-Vpr and a dimerization mutant VC-Vpr, the QΔ44 mutant showed a similar percentage of positive cells and the A30L mutant showed 10.52% positive cells.

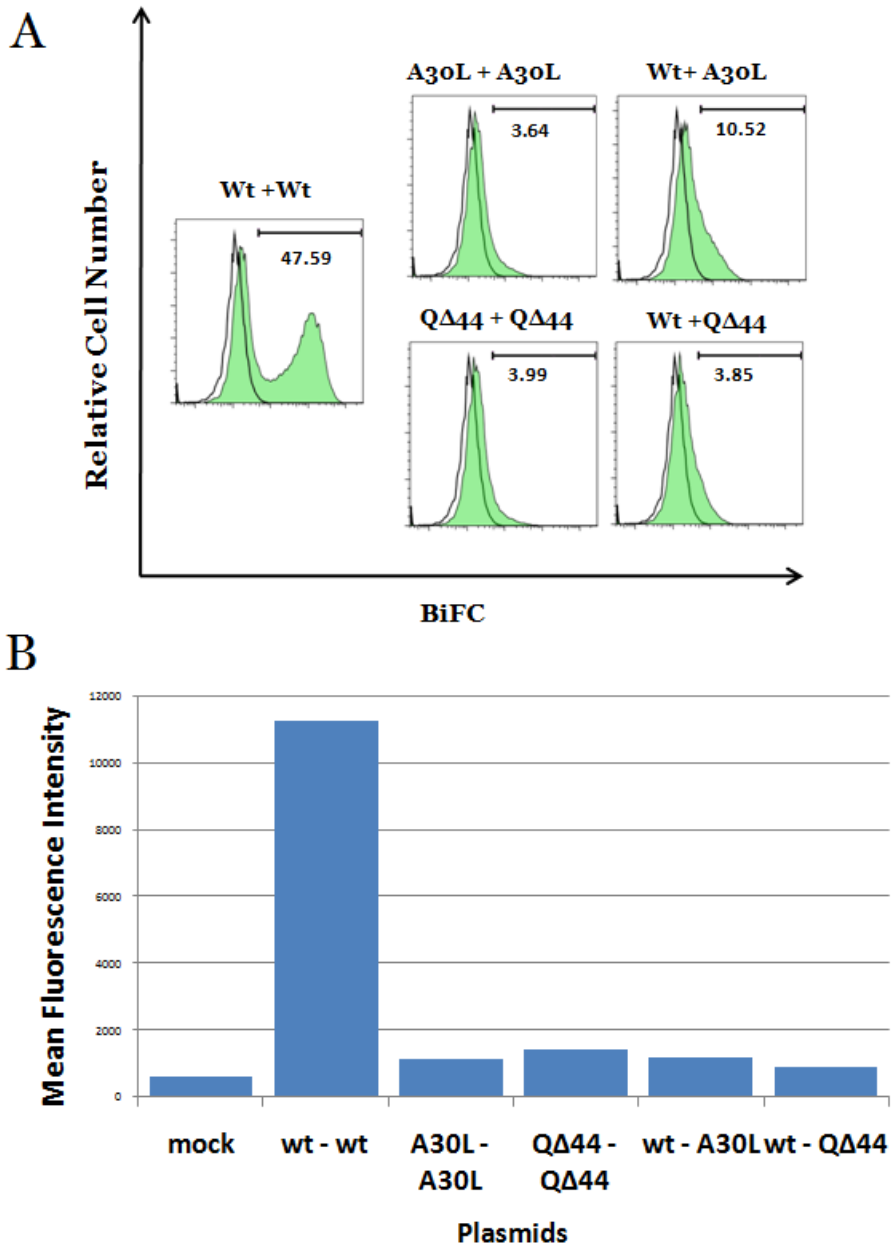

Figure 11: BiFC signal in dimerization-deficient Vpr mutants by flow cytometry. Cells were transfected with VN- and VC- plasmids and collected for flow cytometry analysis 24 hours post-transfection. A) Histograms showing the intensity of FITC signal. (Black line = control cells; shaded = mutant) B) The mean fluorescence intensities from each sample.

Since there is a consistent population of BiFC-positive cells, it is important to consider the degree to which they are positive. In flow cytometry, a cell is excited with a laser and the total fluorescence intensity for that cell is measured. The histograms are comprised of the distribution

of individual cell fluorescence intensities. In the dimerization mutant samples, the histograms are widened and shifted slightly to the right. None of these samples shows the second (positive) peak that is apparent in the wildtype VN- and VC-Vpr histogram. To confirm this, we looked at the mean fluorescence intensity of the entire sample (Fig. 11B). The mean fluorescence intensities of the positive cells in the wildtype VN- and VC- transfection are ten times as high as those of the dimerization mutant pairings, and the mutants' intensity levels are equivalent to the "mock" non-transfected cells.

In HeLa cells, we have found that the BiFC system produces non-specific interactions in 10-20% of cells, but the flow cytometry indicated that the interactions themselves are of low intensity, meaning they occur infrequently within a single cell. We assessed the intensity of BiFC signal in context of a high content imaging system (Figure 12). A total of 45 high content images for the Vpr^{A30L} and $Vpr^{Q\Delta44}$ mutants were analyzed for fluorescence in the FITC channel. No nuclear fluorescence can be observed in either mutant. In the Vpr^{A30L} mutant, a few cells can be seen with low level cytoplasmic fluorescence; however, the fluorescence pattern is distinct from that of true BiFC interactions. In an imaging-based system, this level of background is all but undetectable.

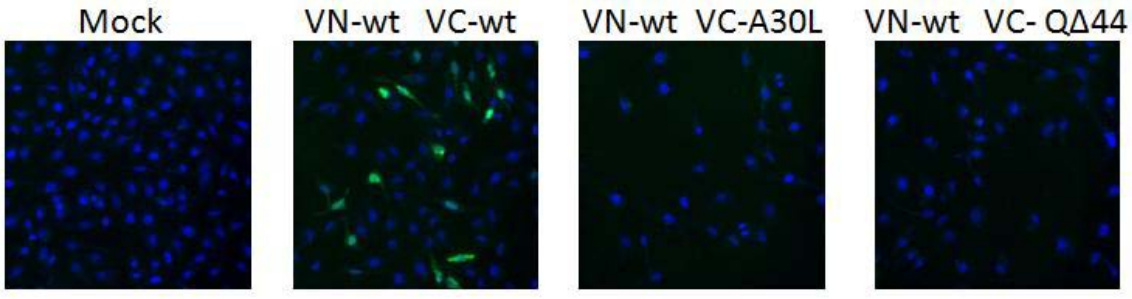

Figure 12: BiFC signal in dimerization deficient mutants by fluorescence microscopy. Cells were transfected with VN- and VC- plasmids for 5 hours, then moved into a 96 well plate. 24 hours post-transfection, cells were fixed, stained and imaged using high content analysis.

5.1.6 Summary of Aim #1

The focus of Aim #1 was to characterize the bimolecular fluorescence complementation system for Vpr oligomerization. Optimal cell lines and transfection reagents were determined in order to conduct all the following assays. The kinetics of BiFC protein expression were explored in order to determine the time by which exogenous compounds must be added in screening experiments. The nuclear localization of individual Venus plasmids and BiFC signal was observed and will be the target of our high content analysis. Furthermore, dimerization deficient mutants were found to produce a consistent, low level BiFC signal that is similar in intensity to non-transfected cells.

5.2 AIM #2: TO QUANTIFY A DECREASE IN FLUORESCENCE USING A COMPETITION ASSAY

5.2.1 Competition Assay Theory

In Aim #1 we showed that the BiFC system can detect Vpr oligomerization. However, in order to function as a screening tool, the BiFC system must be able to quantitatively detect changes in oligomerization levels. Ideally we would use an increasing concentration of a Vpr-specific dimerization inhibitor, but no such inhibitor has been identified. Without this inhibitor, we chose to take advantage of the bimolecular nature of the BiFC system in designing a proof-of-concept assay.

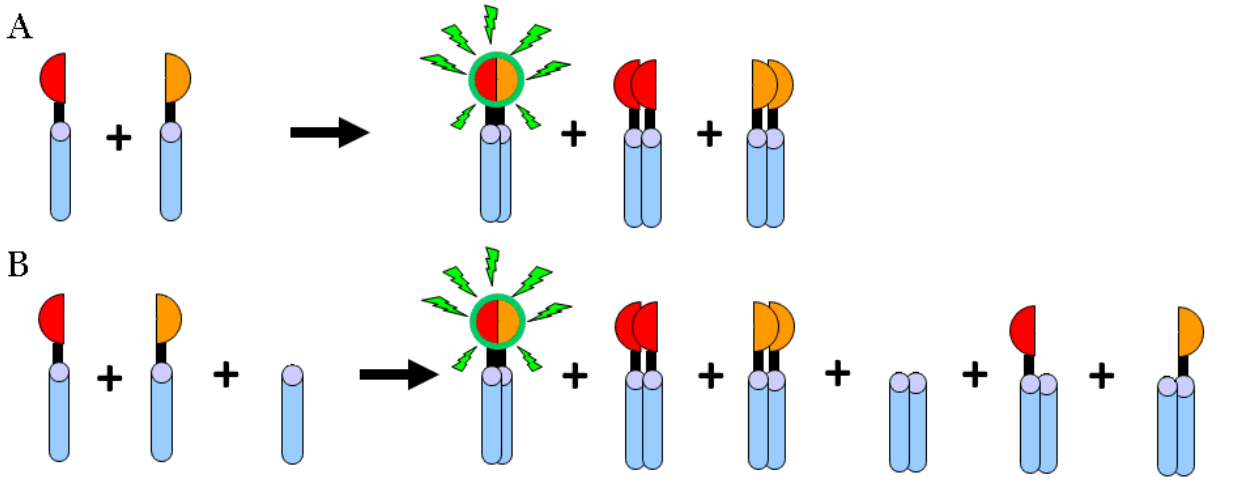

Figure 13: Schematic representation of the BiFC competition assay. Transfection of fusion-less Vpr along with the VN and VC plasmids increases the amount of non-fluorescent dimerization products.

Vpr dimerizes regardless of which fusion protein is attached to it. In every BiFC co-transfected cell, three sets of dimers will be present: VN-Vpr + VC-Vpr, VN-Vpr + VN-Vpr, and VC-Vpr +VC-Vpr (Fig. 13A). Of these three sets, only the VN-VC dimers produce BiFC fluorescence. By expressing Vpr without an attached fusion protein, we double the total number of possible configurations dimerized Vpr can assume (Fig. 13B). By increasing the amount of untagged Vpr transfected into each cell, the percentage of dimers formed in the BiFC configuration is decreased.

We devised ratios to represent the total input of Venus plasmids and untagged Vpr. The total input of Venus plasmids (referred to as "Venus-Vpr") was calculated as the sum of VN-Vpr and VC-Vpr DNA transfected per well. The untagged Vpr input was determined in relation to the amount of Venus-Vpr transfected in order to achieve a given ratio. As an example, a 1-to-4 ratio with a 200ng Venus-Vpr input would be co-transfected with 800ng of untagged Vpr.

One limiting factor of this approach was the maximum amount of DNA that could be tolerated by cells. According to the manufacturer's protocol for PolyJet transfection, a total of 1µg of plasmid DNA was recommended. Experimentally, we found that up to 2µg could be transfected without increasing cytotoxicity. However, even this amount of plasmid was found to be a limiting factor in achieving higher ratios of Venus-Vpr to untagged Vpr. A 1-to-10 ratio was the highest attempted.

5.2.2 HA-Vpr as an untagged competitor

We first attempted to use a construct of Vpr tagged at the N-terminus with an HA epitope (referred to as HA-Vpr) as our untagged competitor. We used a total of 2µg for each sample and adjusted the inputs of both Venus-Vpr and HA-Vpr to reflect the desired ratio (Table 5).

Table 5: Transfection scheme with variable inputs of Venus-Vpr

Ratio	Venus-Vpr (µg)	HA-Vpr (µg)
1 : 0	2	--
1 : 1	1	1
1 : 2.5	0.66	1.34
1 : 5	0.4	1.6
1 : 10	0.2	1.8
0 : 1	--	2

Samples were transfected with the plasmid ratios described above and analyzed via flow cytometry 24 hours post-transfection. Both the percentage of BiFC positive cells and the mean fluorescence intensity of BiFC positive cells were assessed (Figure 14).

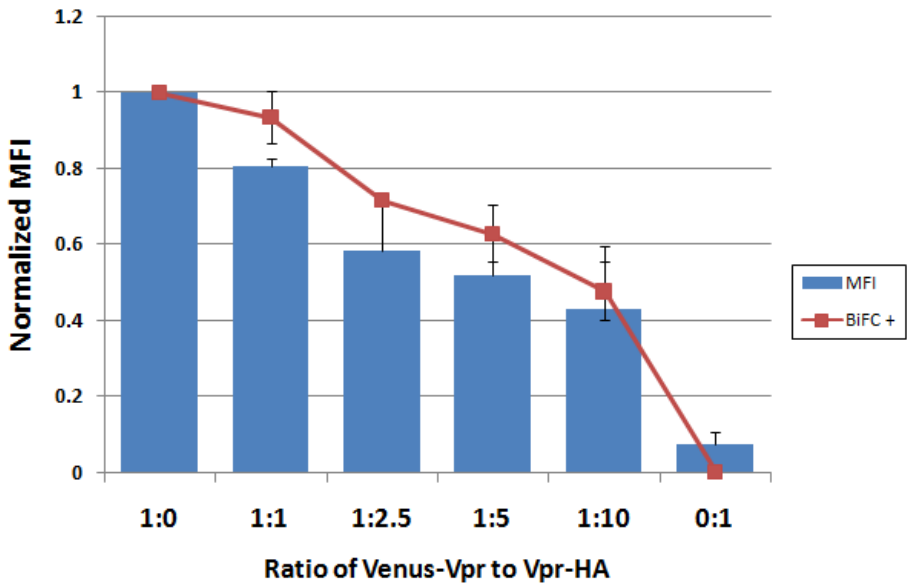

Figure 14: Variable Venus-Vpr input results in non-comparable protein expression levels. Cells were transfected with 2ug of plasmid comprising different ratios of Venus-Vpr to HA-Vpr. 24 hours post-transfection, cells were harvested and analyzed by flow cytometry.

As the amount of HA-Vpr plasmid was increased, a steady decrease in the percentage of positive cells was observed. A decrease of approximately 10% was seen between each ratio, and at a 1:10 ratio the amount of BiFC positive cells had decreased by 50%. A similar linear decrease was seen in the mean fluorescence intensity of BiFC positive cells.

To verify these results, we looked at the protein expression levels in transfected cells by Western blot. The variable input of Venus plasmids resulted in different basal levels of tagged Vpr. Without a way to standardize the different levels, no conclusions can be drawn about the BiFC signal between these samples. Venus plasmid input must be held constant in order to compare the effect of increasing the untagged Vpr.

We next held the amount of Venus-Vpr constant at 400ng (200ng of VN-Vpr and 200ng of VC-Vpr). Control pcDNA3.1 plasmid was added as needed so the total amount of plasmid transfected was 2µg (Table 6).

Table 6: Transfection scheme with constant level of HA-Vpr.

Ratio	Venus-Vpr (µg)	HA-Vpr (µg)	pcDNA vector (µg)
1 : 0	0.4	--	1.6
1 : 1	0.4	0.4	1.2
1 : 2	0.4	0.8	0.8
1 : 4	0.4	1.6	--
0 : 1	--	0.4	1.6

The new transfection scheme was assessed for protein expression by Western blot (Figure 15). The levels of Venus plasmids were equivalent in each of the sample lanes. However, the HA-Vpr expression was lower than that of VN-Vpr and VC-Vpr, even at four times the plasmid input. 200ng of VN-Vpr and VC-Vpr plasmids produced levels of protein higher than 1.6µg of HA-Vpr. The HA-Vpr plasmid was prepared fresh from a glycerol stock, subcloned, re-purified, and tested five times with similar results. Because of the low expression and 2µg limit for plasmid DNA input, we chose to switch to another construct for our untagged Vpr.

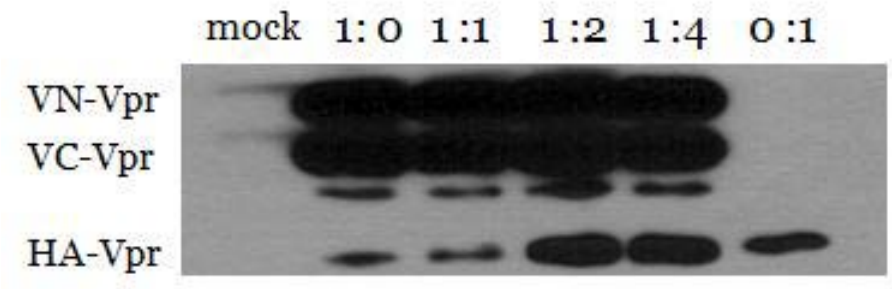

Figure 15: HA-Vpr expression is suboptimal. Cells were transfected as described in Table 6 and ollected after 24 hours for Western blot analysis using α-HA antibody.

5.2.3 Vpr-Flag as an untagged competitor

Since the HA-Vpr plasmid was not capable of high expression, we switched to a construct of Vpr tagged at the C-terminus with a Flag epitope (Vpr-flag) as the untagged competitor. In addition, the amount of Venus-Vpr was decreased to 200ng (100ng of VN-Vpr and 100ng of VC-Vpr). Control pcDNA3.1 plasmid was added as needed so the total amount of plasmid transfected was 2μg (Table 7).

Table 7: Transfection scheme for Vpr-flag competition assay.

Ratio	Venus-Vpr (μg)	Vpr-flag (μg)	pcDNA vector (μg)
1 : 0	0.2	--	1.8
1 : 1	0.2	0.2	1.6
1 : 2	0.2	0.4	1.4
1 : 4	0.2	0.8	1.0
1 : 8	0.2	1.6	0.2
0 : 1	--	0.2	1.8

As before, cells were transfected and observed 24 hours post-transfection. In sample wells with a high input of Vpr-flag plasmid, apoptosis/cell death was observed. Therefore, we reduced the end point to 18 hours post-transfection to avoid time-dependent toxicity. Cells were harvested for flow cytometry and analyzed for percentage of BiFC positive cells and mean fluorescence intensity of BiFC positive cells (Figure 16). The graphs in Figure 16 represent the averages over 4 experiments. The values in each experiment have been normalized to the 1:0 sample, which was taken to be 1.

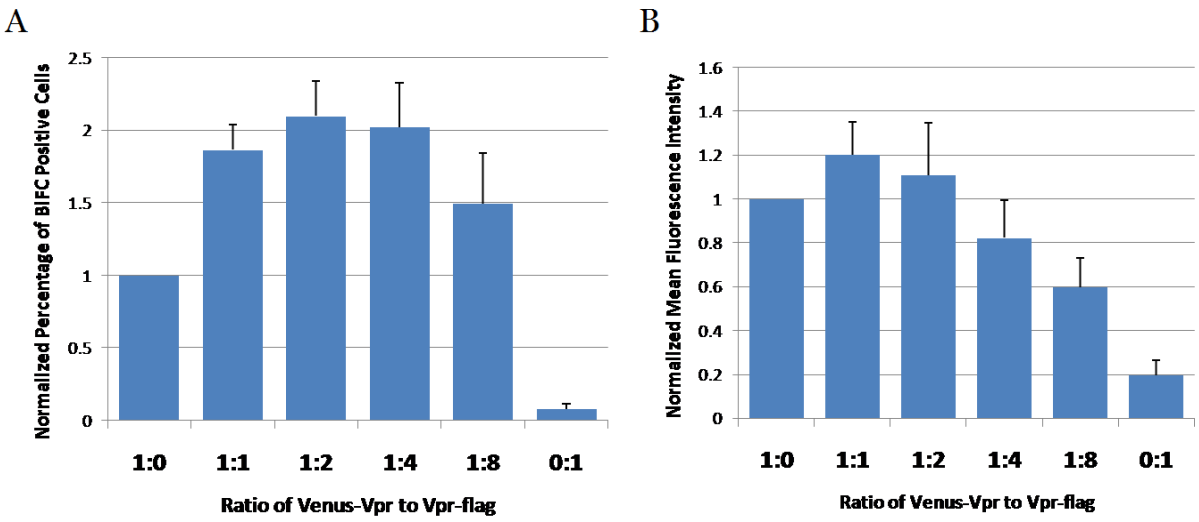

Figure 16: High concentrations of Vpr-flag decrease the mean fluorescence intensity. Cells were transfected as described in Table 3 and collected for flow cytometric analysis 18 hours post-transfection. Experiments were repeated (n=4) and the data from each were normalized to the 1:0 sample. **(A)** The percentage of BiFC positive cells and **(B)** the mean fluorescence intensity are plotted.

Interestingly, both the mean fluorescence intensity (MFI) and percentage of positive cells increase when Vpr-flag is co-transfected along with the Venus-Vpr plasmids. The percentage of positive cells increases by 65%, and the MFI increases by 30%. After this initial increase, the percentage of BiFC positive cells remains constant, and the MFI decreases. These results are seen with a Venus-Vpr plasmid input of 400ng as well (data not shown). This may be due to higher order oligomerization as opposed to dimerization.

The mean fluorescence intensity (MFI) shows an initial spike with the co-transfection of untagged Vpr, but decreases steadily afterwards. The level is reduced to that of Venus-Vpr alone at a ratio of 1-to-4, and is decreased to 70% of the Venus-Vpr alone level at the 1-to-8 ratio. Visually, these decreases can be seen in the histograms for BiFC fluorescence (Figure 17).

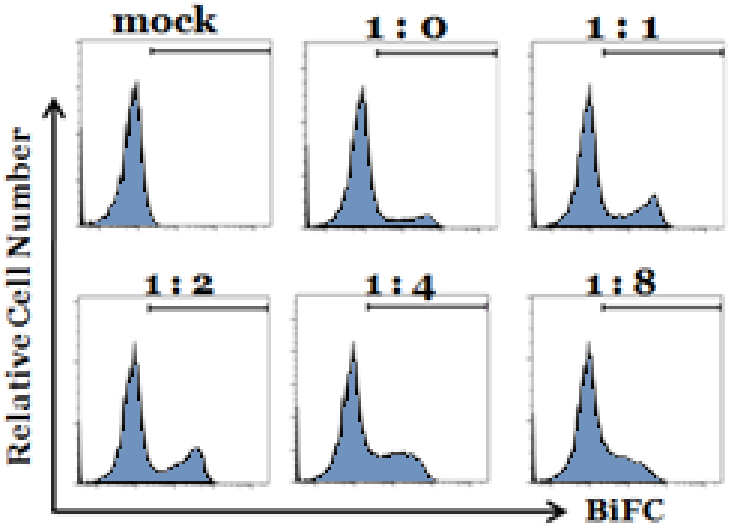

Figure 17: Co-transfection of Vpr-flag produces a re-distribution in the histogram shape. Cells were transfected as described in Table 7 and collected for flow cytometric analysis 18 hours post-transfection. The histograms of the BiFC intensity are shown.

At the 1-to-4 and 1-to-8 ratios, the positive peak has shifted to the left. Since the percentage of BiFC positive cells remains constant, it is unlikely that this shift is due to a change in the expression of the BiFC plasmids. To verify the level of expression in these samples, we performed a Western blot on cell lysates from these co-transfected cells (Figure 18).

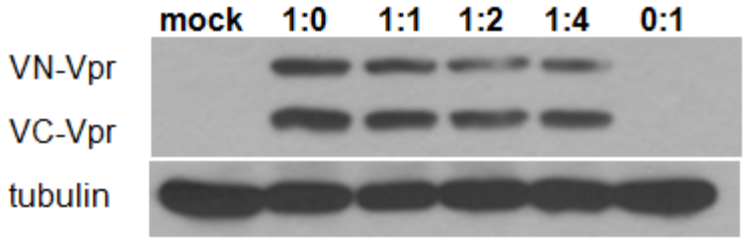

Figure 18: Protein expression in Vpr-flag competition assay. Cells were transfected as described in Table 7 and collected 18 hours post-transfection for Western blot analysis using α-HA antibody.

The expression of VN-Vpr and VC-Vpr is equivalent in all the cell lysates. With no change in Venus-Vpr protein expression between the samples, the shift to the left of the histograms in the 1-to-4 and 1-to-8 samples cannot be attributed to variation in expression or translation. We calculate the mean fluorescence intensity using only the BiFC positive population, so the

percentage of BiFC positive cells is not reflected in this measurement. A change in strength/intensity of the BiFC signal of individual cells is the most likely explanation of the decrease seen in the MFI and histograms.

We next assessed the decrease in BiFC signal intensity using immunostaining followed by imaging using a confocal microscope. In order to clearly visualize the differences, the 1-to-8 ratio of Venus-Vpr to Vpr-flag was used. HeLa cells were grown on coverslips and transfected with 100ng Venus-Vpr plasmids (50ng VN-Vpr and 50ng VC-Vpr) with or without Vpr-flag, fixed, and stained with anti-Flag antibody (Figure 19).

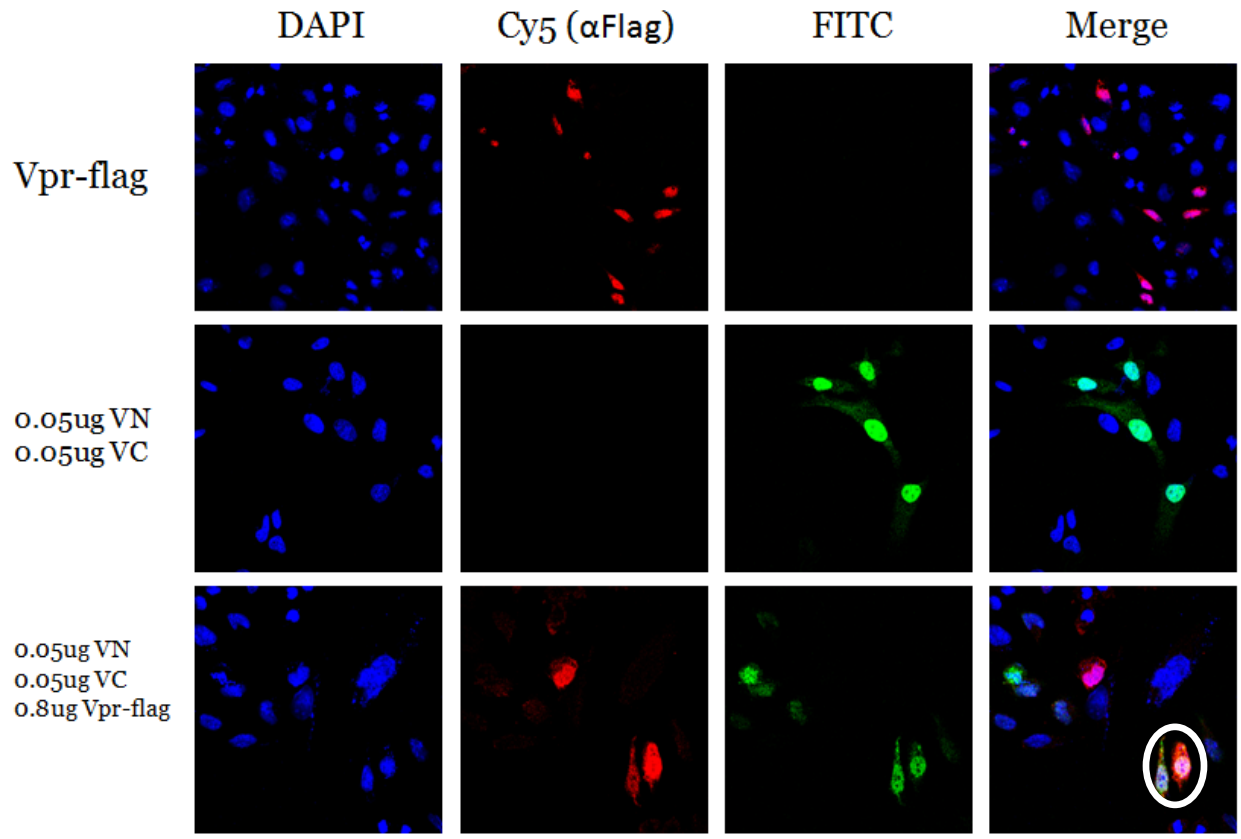

Figure 19: Fluorescence intensity decreases with the co-transfection of Vpr-flag. Cells were seeded onto coverslips and transfected as described. Coverslips were fixed at 20 hours post-transfection, stained with monoclonal Flag M5 and Cy5-conjugated secondary antibodies, and viewed with a confocal microscope at 60X magnification.

The FITC laser PMT was set at a constant voltage of 790 for all images taken in this set to ensure an accurate comparison. A visible decrease in BiFC fluorescence intensity was observed in all cells co-transfected with Vpr-flag compared with Venus-Vpr alone. A representative set of Venus-Vpr and Vpr-flag co-transfected cells is shown circled in white on the merged image. The differences in BiFC intensity were quantified using MetaMorph software. The average intensity of FITC signal in the nucleus for Venus-Vpr transfection without Vpr-flag (n=4) was 223.34 ± 47.09. For Vpr-flag co-transfected cells, five separate images containing n=12 co-transfected cells were analyzed to generate an average pixel intensity of 141.10 ± 22.85. When we normalized to the Venus-Vpr transfection, we found a 37% decrease in pixel intensity. Using flow cytometry, we saw a decrease of 30% from Venus-Vpr alone to the 1:8 sample. These results complement each other and show that a decrease in oligomerization can be visualized by both flow cytometry through mean fluorescence intensity of BiFC positive cells and fluorescence microscopy through pixel intensity.

5.2.4 Summary of Aim #2

The focus of Aim #2 was to quantify a decrease in oligomerization using bimolecular fluorescence complementation. A proof-of-concept experiment was designed that takes advantage of the bimolecular nature of the assay, and two expression plasmids were tested under this system. HA-Vpr was unable to achieve the desired levels of protein expression, and Vpr-flag was used for the final assay. The co-transfection of Vpr-flag produces an initial spike in mean fluorescence intensity of BiFC-positive cells, which then steadily decreases as the Vpr-flag concentration is increased. The decrease was not attributable to protein expression levels and

could be visualized by a shift to the left in the flow histogram and by a decrease in pixel intensity in immunofluorescence analysis.

5.3 AIM #3: TO ASSESS LIBRARIES FOR AN EFFECT ON VPR OLIGOMERIZATION

5.3.1 Initial Toxicity Assessments

As shown in section 5.1.1.2, cells undergo considerable stress during this assay. The addition of an exogenous small molecule will cause additional stress to cells. To ensure that treatment with peptide and small molecules was not going to lead to toxicity, it was necessary to optimize two parameters: the volume of solvent added into the media and the final small molecule concentration in the media.

5.3.1.1 Volume of DMSO Solvent

Some Vpr peptides and all leucine rotamers were dissolved in DMSO, and high concentrations of DMSO are toxic to cells. In order to determine the maximum volume of compound that could be added to cells, it was first necessary to test the quantity of DMSO that transfected HeLa cells could tolerate. A cytotoxicity assay was performed on transfected cells treated with increasing volumes of DMSO (Figure 20). Cell survival was decreased by 15% with the addition of 1μL DMSO, and to 20% with the addition of 5μL, whereas 10μL resulted in 80% cell death. We elected to use a solvent volume of 2μL when adding peptides and small molecules to wells so

that no greater than 20% of cells would be affected by the DMSO solvent alone. With a solvent volume of 2µL added into 200µL of media, library members undergo a final dilution of 1 to 100.

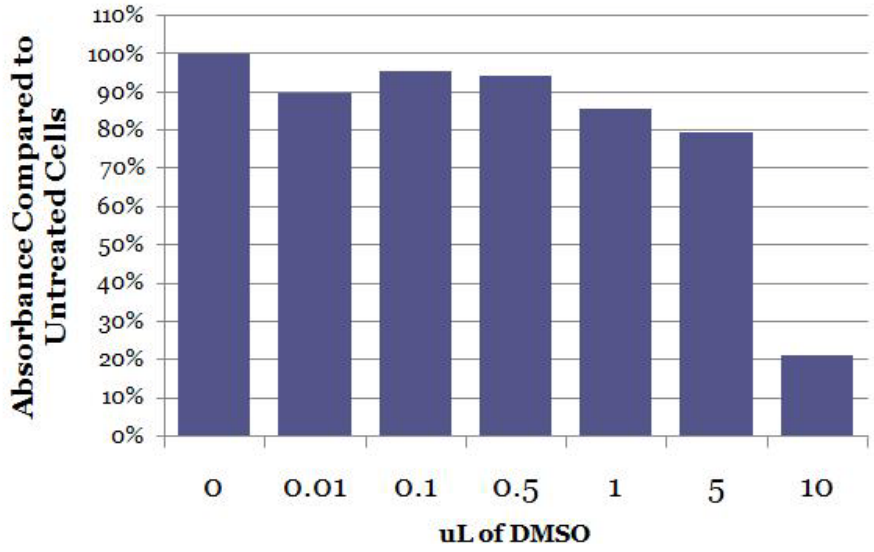

Figure 20: DMSO tolerance of transfected HeLa cells. Five hours post-transfection, cells were transferred to a 96 well plate and DMSO was added to wells in triplicate. At 24 hours post-transfection, cytotoxicity was assessed by MTT assay.

5.3.1.2 Concentration of Peptide Library

We next determined the maximum concentration of the Vpr peptide library that transfected cells could tolerate. Vpr peptides were dissolved according to the solubility table in Appendix A and reconstituted to a concentration of 1 mg/mL, which is the equivalent of 500-600 µM. A final concentration of 10 µg/mL of peptide was tested for cell survival by MTT assay (Figure 21).

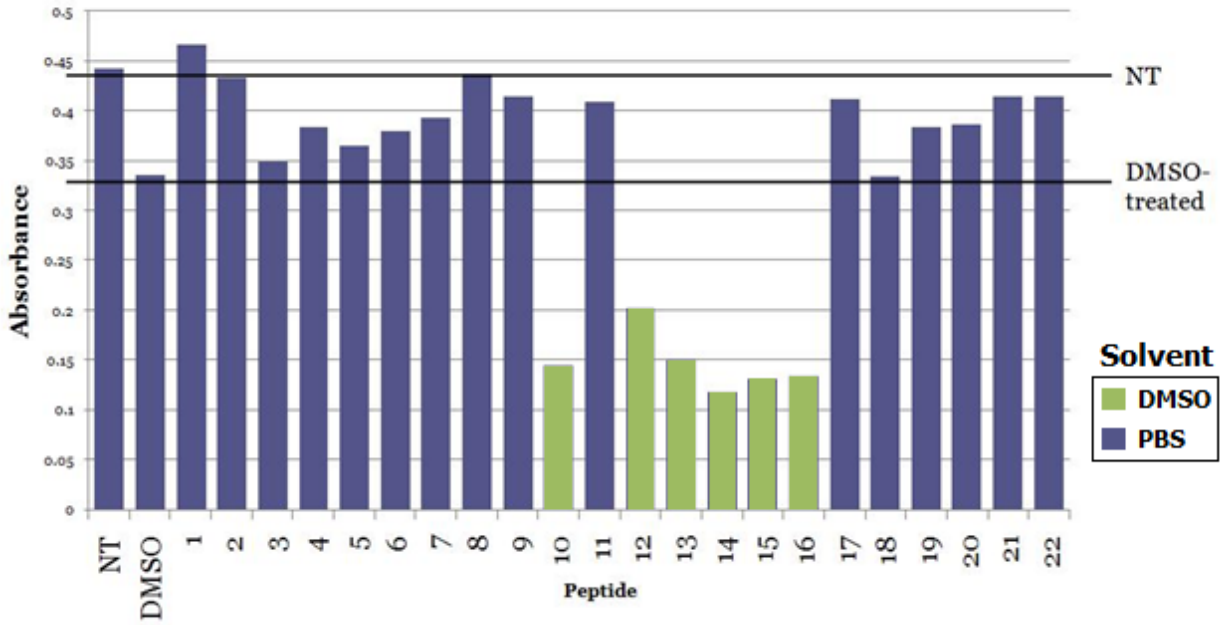

Figure 21: Cytotoxicity of peptide library at 10 µg/mL. Transfected cells were treated in triplicate with peptide at a concentration of 10 µg/mL and analyzed by MTT assay 24 hours post-transfection. Blue bars represent peptides dissolved in PBS, and green bars represent peptides dissolved in DMSO.

No toxicity greater than 20% was seen in the peptides dissolved in PBS. These peptides were assayed at a final concentration of 10 µg/mL in all subsequent experiments. DMSO-mediated toxicity decreased cell survival by 25%. Even when normalized to the DMSO-treated control, peptides 10 and 12-16 exhibited greater than 50% toxicity. These peptides were diluted 1:10 into DMSO to maintain solubility and tested at a final concentration of 1 µg/mL (Figure 22).

At 1 µg/mL, no toxicity beyond that attributable to the DMSO solvent was observed in peptides 10 and 12-15. Peptide 16 showed 25% toxicity compared to the DMSO-treated cells, and 60% compared to the untreated cells. As this was the only peptide that showed toxicity at 1 µg/mL concentration, we chose to assess the DMSO peptides at the uniform concentration of 1 µg/mL. To control for the difference cytotoxicity of the two solvents, the peptides dissolved in PBS were

normalized to the untreated control, and the peptides dissolved in DMSO were normalized to the DMSO-treated control in all future experiments.

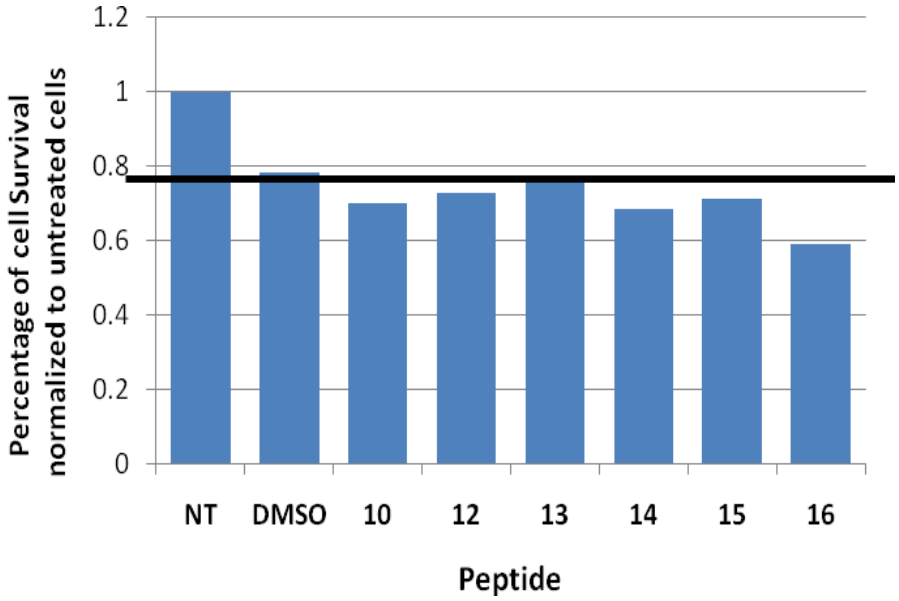

Figure 22: Cytotoxicity of DMSO-dissolved peptides at 1 µg/mL. Transfected cells were treated in triplicate with peptide and analyzed by MTT assay 24 hours post-transfection.

5.3.1.3 Concentration of Leucine Rotamer Library

We next determined the maximum concentration of the leucine rotamer library. We received this library of 45 small molecules as 10mM stocks dissolved in DMSO. Cytotoxicity was assessed at final concentrations ranging from 100nM to 10µM, and 1µM was found to be the highest concentration tolerated (Figure 23).

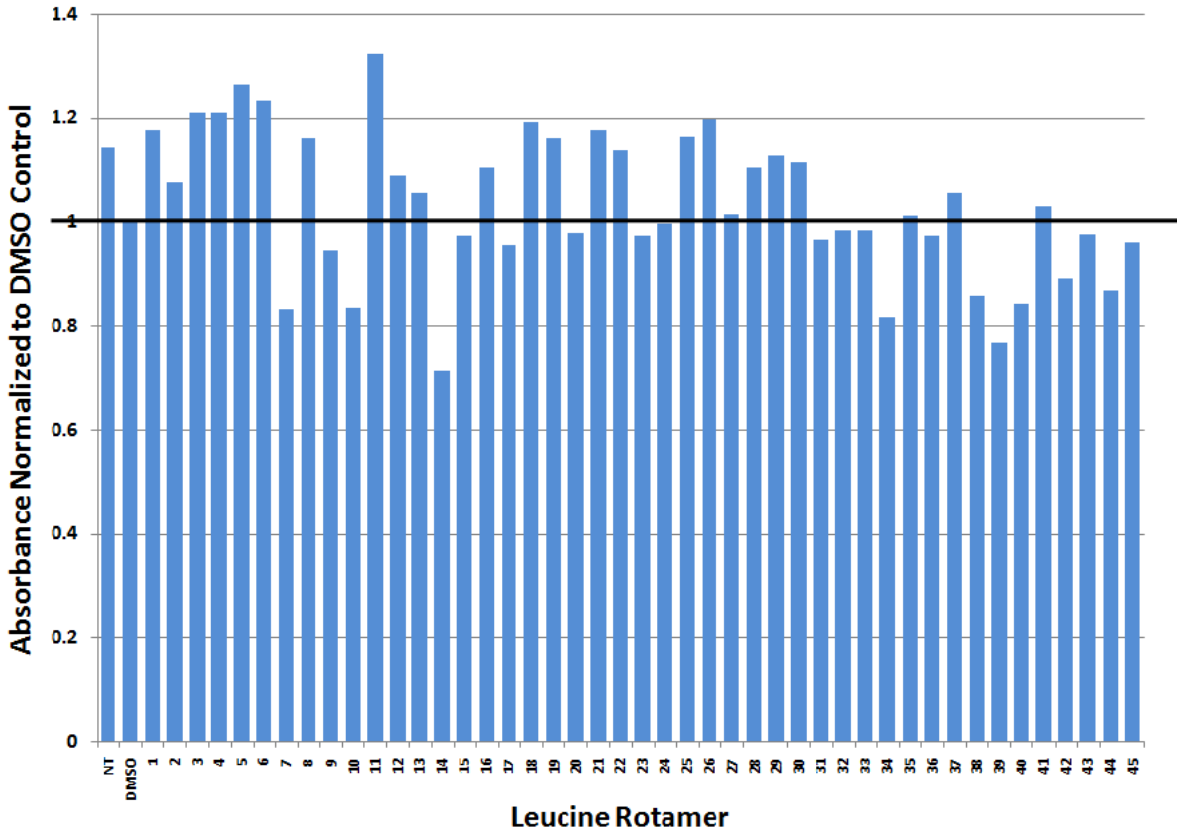

Figure 23: Cytotoxicity of leucine rotamer library at 1 µM. Cells were transfected, transferred to 96 well plate and treated with 1uM of leucine rotamer. 24 hours post transfection, cells were assessed for toxicity using the MTT assay. Absorbance was normalized to the DMSO control, which was taken to be 1. This figure represents one of 3 independent experiments.

There was less than 20% difference between the untreated control and the DMSO control as expected. Relative to the DMSO control, only 5 of the 45 rotamers showed greater than 15% toxicity. An addition 1:10 dilution of these five molecules was performed (for a final concentration of 100nM) but dilution did not significantly increase the cell survival (data not shown). Therefore the leucine rotamer library was screened at a concentration of 1µM per well.

5.3.1.4 Assay Parameter Summary

HeLa cells were transfected in a single plate. Five hours post-transfection, cells were moved and re-plated into a 96 well plate. Cells were allowed to settle for 15 minutes, then treated with library members in triplicate and incubated overnight. Twenty-four hours post-transfection, cells were prepared for analysis by flow cytometry or high content image analysis. Peptides dissolved in PBS were added to cells at 10 µg/mL (5-6 µM), and peptides dissolved in DMSO were added at 1µg/mL (500-600nM). Leucine rotamers were added at 10µM concentrations.

5.3.2 Flow Cytometry Analysis

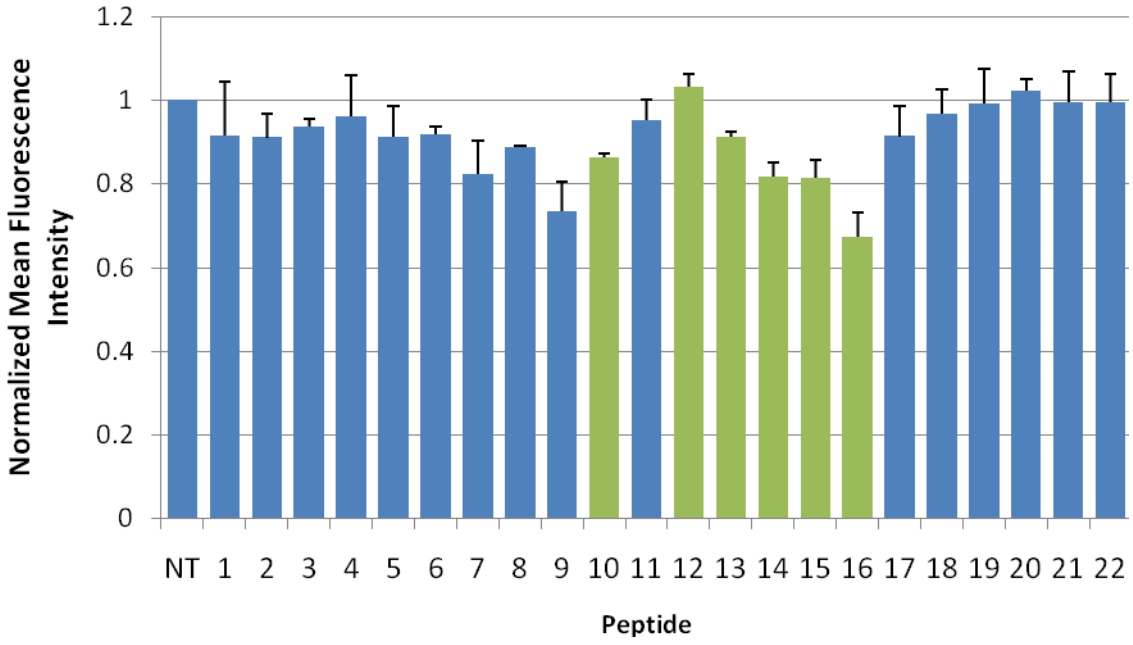

Figure 24: Mean fluorescence intensity of peptide-treated cells. Cells were transfected and treated with peptide in triplicate at 5 hours post-transfection. Cells were prepared for flow cytometry at 24 hours post-transfection. The screen was repeated n=3 times.

We started out screening the overlapping Vpr peptide library. Flow cytometry was used to generate preliminary data. The mean fluorescence intensity of BiFC-positive cells was determined and normalized to the proper solvent control (Figure 24). A greater than 20% reduction in BiFC signal was observed with peptides 9 and 16. However, this decrease is directly correlated with an increase in the total cells positive for BiFC fluorescence. Furthermore, the samples with an increased percentage of positive cells were the result of sample-wide shifts in the fluorescence intensity (Figure 25).

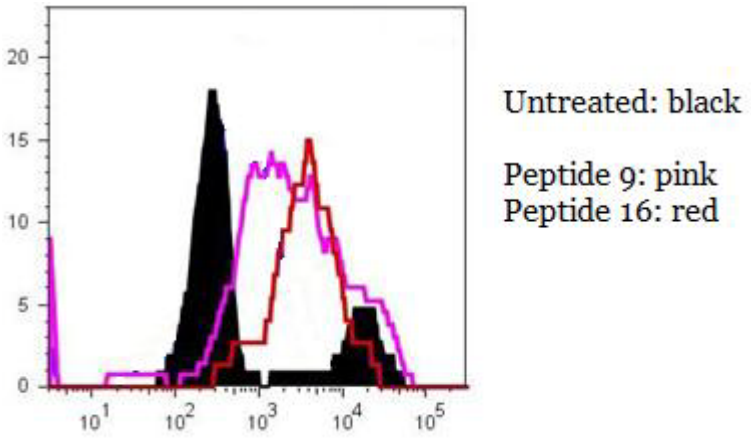

Figure 25: Histogram shifts of two peptides. The fluorescence intensities for all the cells were plotted to obtain the histogram. Peptide 9 is shown in pink and peptide 16 is red.

The peptides caused a shift to the right of over a log in the negative peak. The positive peak was undetectable, but the shifted histogram may just have positive cells that are higher than the detection limit of the flow system (an upper limit of 10,000). The peptides that caused histogram shifts were found to precipitate and fall out of solution upon addition to cell media, and it is likely that the histogram shift is related to this solubility concern. These peptides were reconstituted fresh from lyophilized protein and were found to be soluble once more. They were aliquoted to reduce the need for multiple freeze/thaw cycles.

5.3.3 High Content Imaging Analysis

In attempts to re-test the newly soluble peptides and screen the leucine rotamer library, it became clear that high throughput cytometry was not ideal for running large volumes of large cells. The plate reader function of the BD LSRII cytometer contains narrower tubing than the rest of the machine, and the tubing routinely became clogged mid-way through a plate. On some occasions the machine became completely jammed, and on others the cell counts would vary by over 100% as a clump of cells worked its way free. These data sets were disregarded due to cross contamination of the results from these cell clumps. Between the high run time per plate under ideal (non-clogged) conditions and the frequency of unreliable results, we decided to switch the screening method to a high content image-based analysis.

High content screening uses automated fluorescence microscopy coupled to a CCD camera to do image-based analysis of intensity. Several features make it more convenient than the flow cytometry analysis method, including a shorter run time per plate and less handling of cells before analysis. Cells are fixed in individual wells without the need to prepare a cell suspension. This eliminates the final trypsinization step before flow cytometry, which reduces cell stress and the loss in cell number during centrifugation and washing steps.

5.3.3.1 Z' factor

In order to determine the power of a high content screen, a few variables must be considered. The signal-to-noise ratio measures the resolving power of the assay, or its ability to distinguish positive cells from background fluorescence. The Z' factor measures the separation band, a

combination of the variability and the difference in mean signal between the positive and negative controls [104]. A trial plate consisting of transfected and untransfected cells was analyzed to determine the best measure of intensity in future screens.

The signal to noise ratio (S/N) is calculated as:

$$S/N = \frac{\text{mean signal} - \text{mean background}}{\text{standard deviation of background}}$$

Our test plate showed a S/N of 46.1 using the Average Nuclear FITC Spot Intensity, and a S/N of 8.53 using the Average Nuclear FITC Intensity. The signal-to-noise ratio only shows the resolving power, so it is necessary to also look at the Z' factor, which is calculated as follows:

$$Z = 1 - \frac{3SD \text{ of sample} + 3SD \text{ of control}}{|\text{mean of sample} - \text{mean of control}|}$$

By this definition, our test plate showed a Z' factor of 0.447 using the Average Nuclear FITC Spot Intensity, and a Z' factor of -0.088 using the Average Nuclear FITC Intensity. The negative Z' factor indicates that the separation band is non-existent, either due to resolving power or variation between the sample wells. In this case it is the resolving power that is lacking, as shown by the small S/N obtained for the Average Nuclear FITC Intensity. Desirable Z' factors are in the range of 0.3 to 1. Given the results of these two calculations, the Average Nuclear FITC Spot Intensity was chosen as the measure for BiFC fluorescence in future screening plates.

5.3.3.2 Data Normalization

In order to compare multiple screening plates, each containing replicate wells, a significant amount of data manipulation is necessary. Each small molecule is tested in triplicate on each

plate. The replicate wells were averaged, and the average between these three wells was used to normalize the data between plates.

Based on criteria published by the University of Pittsburgh Drug Discovery Institute, Z scores were used to normalize the data across multiple plates [105]. The Z score is calculated as follows:

$$z = \frac{x - \mu}{\sigma}$$

where x is the value to be normalized, μ is the mean, and σ is the standard deviation of the mean. This calculation expresses the data in terms of the number of standard variations from the mean. For our mean, we use the average across the replicates of the appropriate solvent-treated, transfected control. To compare between plates, we averaged the Z scores from individual plates for each small molecule. Because we were testing a cell-based screen with no known positive control, we set our hit threshold low, requiring standard deviations to fall just one standard deviation above or below the mean in order to consider a molecule as a hit.

5.3.3.3 Analysis of Peptide Library

The overlapping Vpr peptide library was screened n=4 times by high content analysis (Figure 26). Peptides dissolved in DMSO solvent showed a 70% reduction in cell number in comparison to peptides dissolved in PBS (Fig. 26A). While this is a higher level of overall cell loss, the percentage of BiFC-positive cells was constant across all wells (Fig 26B). Despite high toxicity from the peptides, the frequency of BiFC positive cell was the same and thus they are still able to be compared to the rest of the wells.

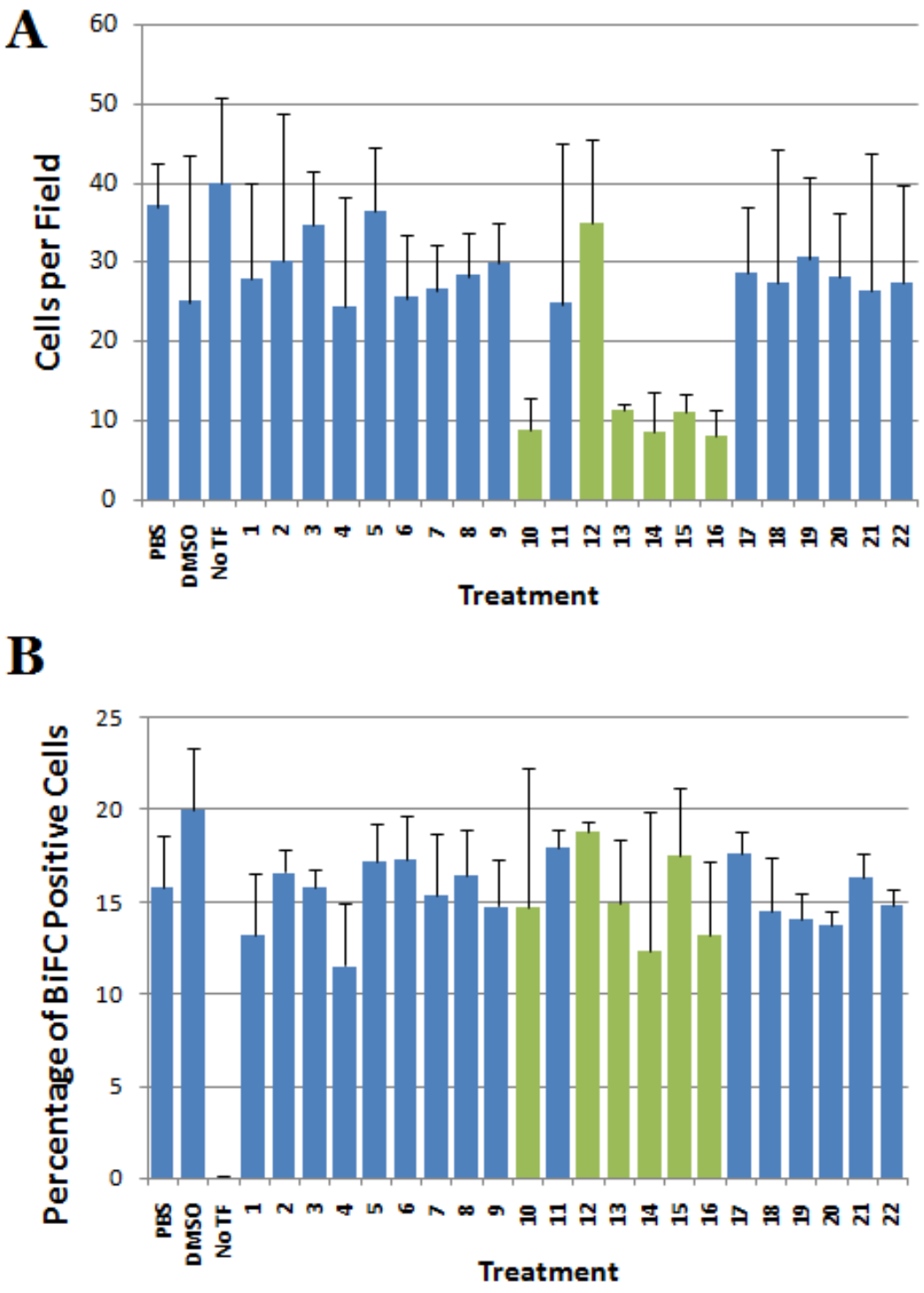

Figure 26: Cell count and BiFC positive cells in high content peptide analysis. Wells were treated with peptide in triplicate and analyzed by high content imaging screen. The (A) total cell count per fluorescence microscopy field and (B) percentage of BiFC positive cells per well from an example plate are shown. Peptides in blue are dissolved in PBS, and peptides in green are dissolved in DMSO.

The library of overlapping Vpr peptides was screened by high content analysis n=4 times. Z scores were calculated and averaged as seen in section 5.3.3.2 and the average scores from 4 repetitions were plotted (Figure 27).

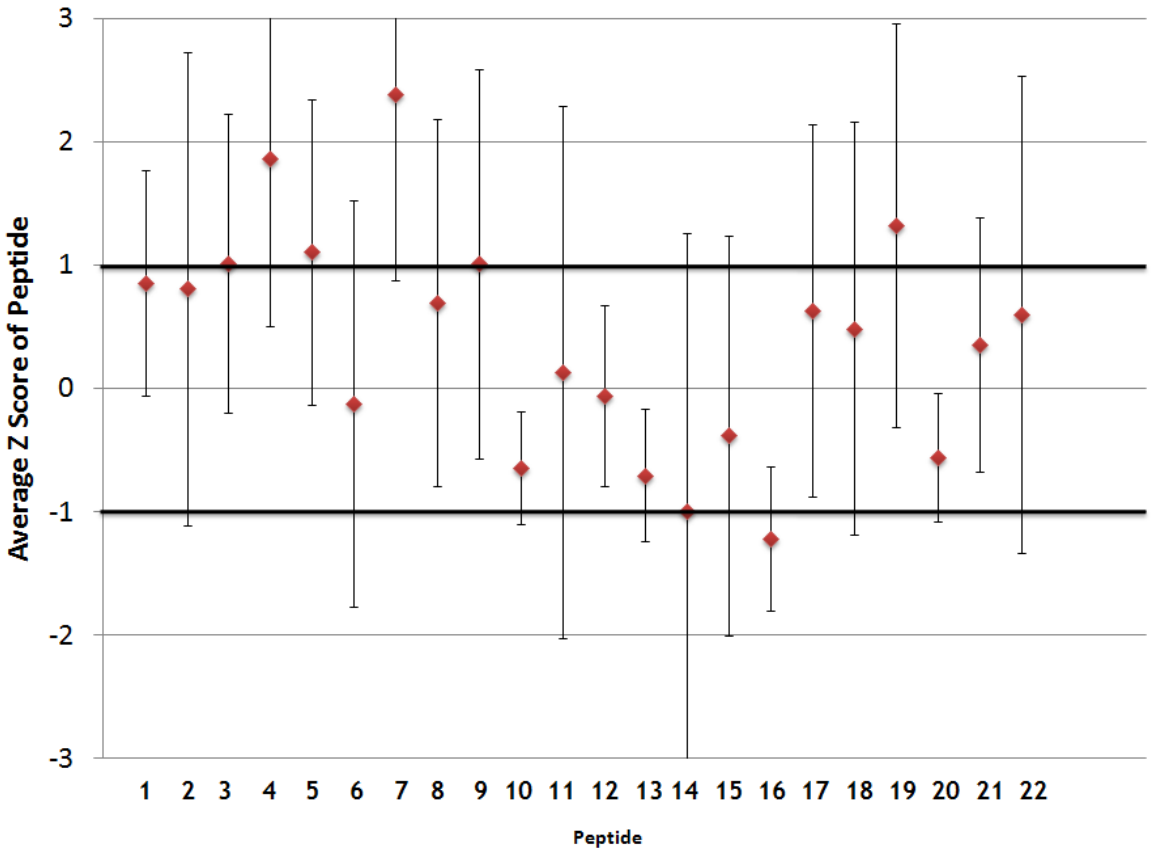

Figure 27: Effect of peptide library on nuclear BiFC signal. Peptides were screened for an effect on nuclear BiFC fluorescence using high content imaging (n=4). Data was normalized to the solvent-appropriate transfected control using Z score methods. The average and standard deviation across 4 repetitions were calculated and plotted.

While five peptides were greater than one standard deviation from the mean BiFC signal intensity, all of their standard deviations overlapped the variability window and thus cannot definitely be considered a deviation from the mean. Analysis by flow cytometry showed that peptides 9 and 16 had the largest negative effect on mean fluorescence intensity of all the peptides. Interestingly, high content analysis showed an increase in nuclear fluorescence

intensity by peptide 9. Peptide 16 was also found to show a negative effect on nuclear BiFC intensity by high content analysis.

5.3.3.4 Analysis of Leucine Rotamer Library

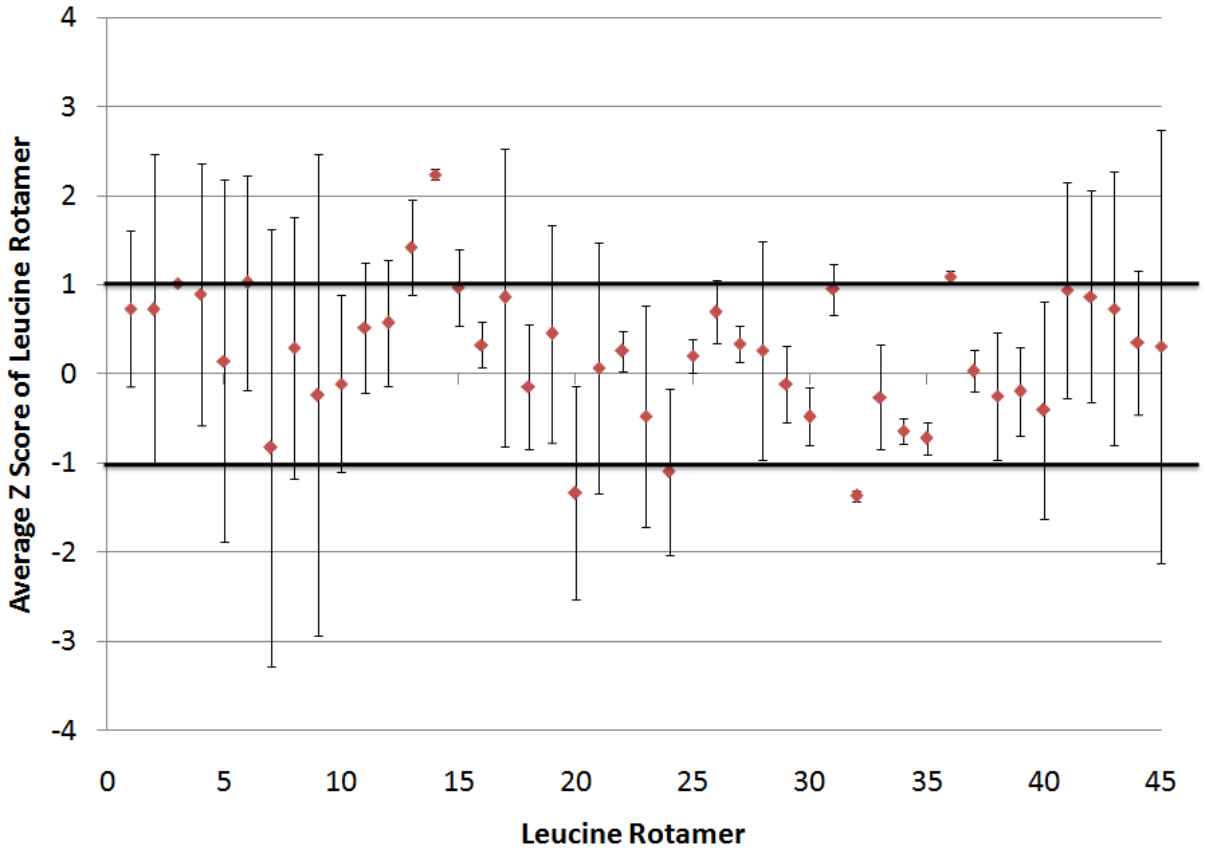

Figure 28: Effect of leucine rotamer library on nuclear BiFC signal. Small molecules were screened for an effect on nuclear BiFC fluorescence using high content imaging (n=2). Data was normalized to the solvent-appropriate transfected control using Z score methods. The average and standard deviation across repetitions were calculated and plotted.

The leucine rotamer library contains 45 small molecules, and it was screened n=2 times using high content image analysis for effects on nuclear BiFC signal (Figure 28). Of the 45 leucine rotamers screened, three had greater than one standard deviation separation from the mean. Rotamer 14 had a separation of +2.23 standard deviations from the transfected control, meaning

it increased the mean nuclear BiFC signal. Rotamer 36 also increased nuclear BiFC signal, but was less potent (separation of +1.09 standard deviation from the transfected control) than rotamer 14. Only rotamer 32 decreased the nuclear BiFC signal by greater than a standard deviation. Rotamer 32 showed a separation of -1.37 standard deviations from the mean.

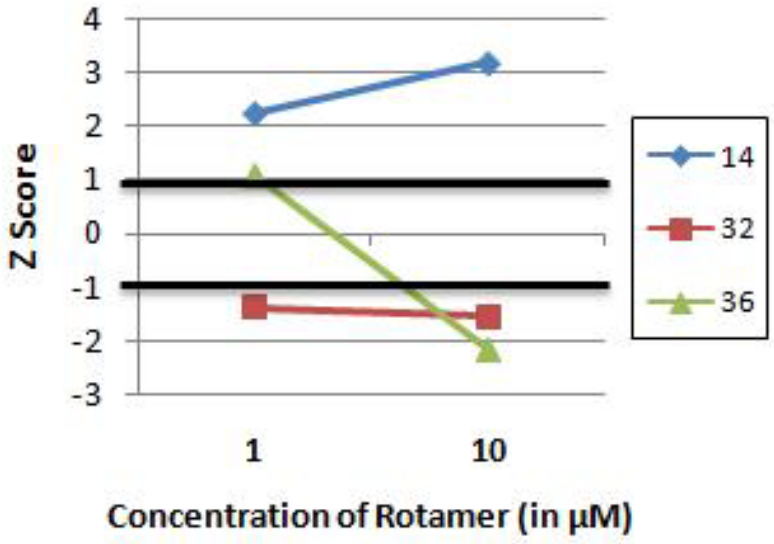

Figure 29: BiFC signal intensity at two concentrations of selected leucine rotamers. Three leucine rotamers were screened for their effect on nuclear BiFC signal at two different concentrations.

These three rotamers were screened again using a 10µM concentration (Figure 29). The positive effect of rotamer 14 on BiFC signal was magnified to greater than 3 standard deviations at 10µM. The negative effect of rotamer 32 remained the same at both concentrations. At the original concentration, rotamer 36 treatment resulted in an increase in nuclear BiFC fluorescence; however, at the higher concentration a negative effect on nuclear BiFC fluorescence was observed. At 10µM, a 67% reduction in cells per field was seen with rotamers 32 and 36. Rotamer 14 is comparatively less toxic, with just a 20% reduction in cells per field.

5.3.4 Summary of Aim #3

Maximum tolerated concentrations of two small libraries were determined using a MTT cell survival assay. The efficacy of the libraries to block Vpr oligomerization was screened using a combination of two methods: plate-based flow cytometry and automated fluorescence microscopy. Flow cytometry was abandoned for technical reasons, and imaging-based high content screening was the final method of analysis. The overlapping Vpr peptide library was screened at 5-6μM for peptides dissolved in PBS, and 500-600nM for peptides dissolved in DMSO, but no peptides showed a significant deviation from the control BiFC signal. The leucine rotamer library was screened at 1μM, and two molecules of interest were identified. One showed a concentration-dependent increase in BiFC signal, and the other showed a decrease in BiFC signal.

6.0 DISCUSSION

After over 25 years of HIV research, scientists still have not discovered a cure for HIV/AIDS. The development of HAART has prolonged the lives of millions of HIV positive patients and has reduced the spread of disease, especially through vertical transmission [106]. However, the inability to follow this toxic and strict drug regimen, in combination with the high mutation rate of HIV-1, leads to the evolution of drug-resistance in patients that ultimately causes HAART to fail and patients to succumb to AIDS-related opportunistic infections.

The HIV-1 genome is composed of 9 genes whose products perform structural, enzymatic and accessory roles in the viral life cycle. HAART targets HIV-1 enzymes and steps involved in replication and entry. Advances in the study of protein-protein interactions (PPI) in the last ten years have opened up new lines of research in the field of HIV therapeutics that have shown promise *in vitro* [17, 41, 56]. One specific type of protein-protein interaction, the formation of dimers, has been identified as a drug target in almost all HIV proteins [39, 42, 53, 61-63, 107].

The HIV-1 accessory protein Vpr is multifunctional and affects several host cellular pathways to enhance viral replication. It arrests the cell cycle at G2/M, induces apoptosis in bystander cells, regulates cellular immune function, causes neuropathogenesis, and is incorporated into new virus particles [76, 78, 80, 82]. Vpr incorporation into viral particles indicates that it plays a role in

early infection. Vpr has been shown to enhance the infection of macrophages, transactivate the viral LTR promoter, and to assist in transport of the pre-integration complex into the nucleus [85, 93, 108]. Without the presence of Vpr in the virion, the early stages of viral replication could be hampered. It has been shown that dimerization-deficient Vpr cannot be incorporated into virus particles. The focus of this thesis was two-fold: First, to develop an assay to measure changes in Vpr oligomerization and secondly, to screen two libraries for inhibitors of Vpr oligomerization.

Our laboratory had previously created a pair of bimolecular fluorescence complementation (BiFC) plasmids for Vpr. When co-transfected, these plasmids produce Vpr fusion proteins that restore a fluorescent molecule when the fusion proteins are in close proximity during dimerization. Initial studies were performed to determine the optimal cell line and transfection reagents with which to visualize this fluorescence complementation. A protocol was devised that routinely transfected over half of HeLa cells with both complementation plasmids (Figure 8). With the basic parameters of the assay in place, we focused on how to test exogenous molecules for an effect on this dimerization.

Our system relies on a large-scale transfection followed by replating into a 96 well plate in order to reduce the well-to-well variation in transfection efficiency that accompanies individual transfections. This strategy has been implemented successfully in the development of other high content screens [109-111]. As the BiFC reaction is irreversible, the timing of the replating and compound addition is critical to the success of the assay [69]. We found that our system yielded protein expression between 6 and 9 hours post-transfection (Figure 10). Replating and the

addition of small molecules were performed at 6 hours post-transfection to ensure that cells had time to take up the compounds before protein expression began.

The next focus of our study was to show that the BiFC system could resolve a decrease in Vpr oligomerization. Dimerization relies on the secondary and tertiary structure of a protein, not specific motifs [65]. As a result, there are no broad-spectrum dimerization inhibitors available, nor any that target a general leucine zipper or beta sheet structure. Small molecule inhibitors of dimerization tend to be discovered through rational design based off of a crystal structure of a protein [112, 113]. There is no crystal structure available for Vpr, nor is there a known inhibitor of Vpr dimerization. Of the eight inhibitors of Vpr functions, only two have been shown to bind directly to Vpr [97, 98].

In order to detect a decrease in Vpr oligomerization through BiFC signal, we used a competition assay. A similar strategy has been used in screening to discover high affinity binders of transcription factors [114]. Using a triple transfection strategy, we co-transfected the two Venus-tagged Vpr plasmids and a Vpr expression plasmid without a BiFC tag. Because all three of the plasmids encode full-length Vpr, more non-BiFC configurations of the Vpr dimer are possible (Figure 13). At higher input levels of untagged Vpr, a decrease in the mean fluorescence intensity (MFI) but not percentage of BiFC-positive cells was observed. This suggested that the transfection efficiency was the same among the samples, but that triple plasmid transfected cells fluoresce less brightly than cells not transfected with competitor Vpr. We confirmed this through immunofluorescence analysis, using the ratio that had given us the highest reduction in MFI

(30%) via flow cytometry. Quantitation of the change in spot intensity on the immunofluorescence images showed a similar decrease in intensity (27%).

Interestingly, the percentage of BiFC-positive cells in triple plasmid-transfected cells was twice that of VC and VN plasmid co-transfected cells (Figure 16A). One possible explanation for this is the formation of higher order oligomers. Between the 1:0 sample and the 1:1 sample, the input of Vpr-encoding plasmid doubles. Vpr is known to form dimers, trimers and hexamers in a concentration-dependent manner [89]. This initial increase was seen regardless of the initial input of Venus-Vpr (tested at 100ng, 200ng, and 400ng).

After verifying the quantitative nature of the BiFC system with a competition assay, it was necessary to determine the volume and concentration of compound that transfected cells could tolerate. HeLa cells tolerated up to 2.5% DMSO in their media, and our screens were designed for a maximum addition of 1% DMSO to the media (Figure 20). The peptide library was split into two sections depending on their solvent (PBS or DMSO). The peptides dissolved in PBS were tolerated at a final concentration of 10μg/mL, or 5-6μM. Peptides dissolved in DMSO were tolerated at a 10-fold dilution, 1μg/mL. The leucine rotamer library was tolerated at a final concentration of 1μM. With these concentrations determined, we started screening using plate-based flow cytometry.

Plate-based flow cytometry was able to provide preliminary data on the peptide library, but mechanical issues with the plate reader prevented further analysis of the leucine rotamer library. Imaging-based high content screening, using automated fluorescence microscopy, has several

advantages over flow-based screening. The preparation for flow involves trypsinization and the generation of a single cell suspension; this is the third trypsinization in 36 hours in this assay protocol. Much less time and labor is needed in the preparation for high content analysis, and the addition of nuclear staining provides a measure of cytotoxicity. In practice, however, toxicity was observed as a decrease in cells per field, not as nuclear fragmentation.

One important feature of a high content screen is the Z' factor. This measurement takes into account the difference between the positive and negative controls in the assay and the variability from well-to-well. A sample plate, consisting of untransfected and transfected cells, was run in the high content system. Knowing that the BiFC signal is localized in and around the nucleus, the list of potential variables was restricted to nuclear FITC intensity. Even with this restriction, there were six sets of values from which to choose. The highest Z' factor was 0.447, and it was obtained using the average nuclear spot FITC intensity. This variable was used to evaluate the remainder of the HCS experiments.

In order to compare multiple plates against each other, the data needed to be normalized. Replicates within a single plate were averaged, and the average was normalized to the solvent-appropriate transfection control. For example, a peptide dissolved in DMSO was normalized to transfected cells treated with 1% DMSO. Z scores were the methodology recommended by the Hillman Cancer Center Flow Cytometry core at which the samples were run and the University of Pittsburgh Drug Discovery Institute [105]. Z scores present the difference between a value and the control in terms of standard deviations from the control mean. The hit threshold of greater than one standard deviation from the mean was chosen for three reasons. First, this is a cell-

based screen and the library members may be impermeable to cells. Secondly, the final concentrations of small molecule that we are applying to cells are in the low micromolar range. *In vitro* HTS assays typically discover hits in the high micromolar or millimolar range. The low concentration of the small molecule treatment may reduce the magnitude of the result. Third, this assay does not have a known positive control, and thus no effective dose is available for reference and/or calibration.

The screen of the peptide library (n=4) yielded 5 compounds whose Z score was greater than one standard deviation away from the mean, but all 5 had large error bars that extended into the hit threshold. The screen of the leucine rotamer library (n=2) yielded three compounds who were greater than one standard deviation from the mean and whose error bars did not cross the hit threshold (Figure 28). These rotamers (**14**, **32**, and **36**) were assessed at a tenfold higher dilution of 10uM to further evaluate the effect of higher concentration.. Rotamers 32 and 36 displayed 67% toxicity at the level, but rotamer 14 remained relatively non-toxic. Rotamer 32 had a negative effect on nuclear BiFC intensity, but increasing the concentration of **32** did not increase the magnitude of the effect.

Interestingly, **14** shows increased nuclear BiFC fluorescence compared to the control, and it responded in a dose-dependent manner when tested at a higher concentration. While this was not the desired outcome of the screen, a compound that increases oligomerization of Vpr could have laboratory relevance. Vpr-EGFP is used to create fluorescently tagged virus particles for studies on viral entry and uncoating. If an increase in Vpr oligomerization results in an increase in

incorporation into the viral particle, this small molecule could be used to increase the overall intensity of fluorescent virions, which would aid imaging studies.

Taken together, a system to detect the oligomerization of HIV-1 Vpr was developed and validated. It is capable of measuring changes in fluorescence intensity through both flow cytometry and high content imaging. We concluded that BiFC is a valid system for detecting interference with oligomerization and moved forward to a small-scale high content screen. A total of 67 members of two libraries were screened for effects on nuclear BiFC intensity, and three small molecules with weak but consistent effects were identified.

7.0 FUTURE WORK

Initial studies on HIV-1 oligomerization using the bimolecular fluorescence complementation reporter system have resulted in the creation of a transfection-based screening assay. Using the HIV-1 Vpr oligomerization assay yielded two compounds that have a weak effect on the nuclear fluorescence intensity of the BiFC signal. To further these screening studies:

A transduction system should be created to deliver the Vpr genes. This delivery system would eliminate two sources of cell stress. There would be no need for transfection and the cells could be seeded directly into a 96 well plate, avoiding the re-plating step. Two lentiviral vectors should be created, one for VN-Vpr and one for VC-Vpr. Pseudotyping with VSV-G envelope would ensure high transduction. The two vectors would have to be mixed and titrated to determine the optimum MOI. By alleviating some of the assay-induced cell stress, small molecules should be able to be tested at higher concentrations without causing toxicity-related cell death.

Two small molecules showed an effect on nuclear BiFC signal intensity during the screening process. The effect should first be verified via flow cytometry and/or immunofluorescence. Then secondary screening should be performed to determine the nature of the effect. The level of Vpr expression in small-molecule treated cells should be determined to rule out an effect on translation. The effect of the small molecules on BiFC signal intensity using Venus plasmids

fused to proteins other than Vpr, such as cJun/Fos should be tested to rule out an effect on restoration of the Venus molecule.

Once these small molecules have been verified, further studies could be performed to assess their effect on various Vpr functions, specifically the incorporation of Vpr into new viral particles. These assays could be done in HEK293T cells through pseudotyping of HIV-1 proviral DNA deficient in Vpr (NL4-3ΔVpr or YU-2ΔVpr) with Vpr in the presence of the small molecule, then collecting the virus and probing for Vpr with specific antibody by Western blot. As Vpr fusions are used to create fluorescent viral particles, a small molecule that shows an increase in Vpr incorporation is as useful as one that shows a decrease.

In addition to testing the effect of the identified small molecules on incorporation, structural analogs of the lead compounds could be synthesized and tested for improved potency in the interference of Vpr oligomerization. Knowledge of the structural motifs that improve or abolish effectiveness can help identify the shape of the region to which the small molecule binds.

APPENDIX

VPR PEPTIDE SEQUENCE AND SOLUBILITY INFORMATION

Peptide #	Amino Acid Sequence	Solubility Data		
		Water	PBS	DMSO
1	MEQAPEDQGPQREPY	+	+	+
2	PEDQGPQREPYNEWT	+	+	+
3	GPQREPYNEWTLELL	+	+	+
4	EPYNEWTLELLEELK	+	+	+
5	EWTLELLEELKSEAV	_	+	+
6	ELLEELKSEAVRHFP	+	+	+
7	ELKSEAVRHFPRIWL	+	+	+
8	EAVRHFPRIWLHSLG	+	+	+
9	HFPRIWLHSLGQHIY	+	+	+
10	IWLHSLGQHIYETYG	_	_	+
11	SLGQHIYETYGDTWA	+	+	+
12	HIYETYGDTWAGVEA	_	_	+
13	TYGDTWAGVEAIIRI	_	_	+
14	TWAGVEAIIRILQQL	_	_	+
15	VEAIIRILQQLLFIH	_	_	+
16	IRILQQLLFIHFRIG	_	_	+
17	QQLLFIHFRIGCQHS	+	_	+
18	FIHFRIGCQHSRIGI	+	+	+
19	RIGCQHSRIGIIQQR	+	+	+
20	QHSRIGIIQQRRARN	+	+	+
21	IGIIQQRRARNGASR	+	+	+
22	QQRRARNGASRS	+	+	+

BIBLIOGRAPHY

1. UNAIDS: **UNAIDS report on the global AIDS epidemic.** 2010.

2. **Life expectancy of individuals on combination antiretroviral therapy in high-income countries: a collaborative analysis of 14 cohort studies.** *Lancet* 2008, **372:**293-299.

3. Walensky RP, Paltiel AD, Losina E, Mercincavage LM, Schackman BR, Sax PE, Weinstein MC, Freedberg KA: **The survival benefits of AIDS treatment in the United States.** *J Infect Dis* 2006, **194:**11-19.

4. Flexner C: **HIV drug development: the next 25 years.** *Nat Rev Drug Discov* 2007, **6:**959-966.

5. Bartlett JA, Fath MJ, Demasi R, Hermes A, Quinn J, Mondou E, Rousseau F: **An updated systematic overview of triple combination therapy in antiretroviral-naive HIV-infected adults.** *AIDS* 2006, **20:**2051-2064.

6. Taiwo B, Hicks C, Eron J: **Unmet therapeutic needs in the new era of combination antiretroviral therapy for HIV-1.** *J Antimicrob Chemother* 2010, **65:**1100-1107.

7. Paton NI: **Treatment interruption strategies: how great are the risks?** *Curr Opin Infect Dis* 2008, **21:**25-30.

8. Chesney M: **Adherence to HAART regimens.** *AIDS Patient Care STDS* 2003, **17:**169-177.

9. Wang X, Yang L, Li H, Zuo L, Liang S, Liu W, Dong Y, Yang S, Shang H, Li J, et al: **HIV Drug Resistance and Associated Factors Among Patients on HAART for One Year at Three Sentinel Surveillance Sites in China.** *Curr HIV Res* 2011, **[Epub ahead of print]**.

10. Finzi D, Hermankova M, Pierson T, Carruth LM, Buck C, Chaisson RE, Quinn TC, Chadwick K, Margolick J, Brookmeyer R, et al: **Identification of a reservoir for HIV-1 in patients on highly active antiretroviral therapy.** *Science* 1997, **278:**1295-1300.

11. Collman RG, Perno CF, Crowe SM, Stevenson M, Montaner LJ: **HIV and cells of macrophage/dendritic lineage and other non-T cell reservoirs: new answers yield new questions.** *J Leukoc Biol* 2003, **74:**631-634.

12. Finzi D, Blankson J, Siliciano JD, Margolick JB, Chadwick K, Pierson T, Smith K, Lisziewicz J, Lori F, Flexner C, et al: **Latent infection of CD4+ T cells provides a mechanism for lifelong persistence of HIV-1, even in patients on effective combination therapy.** *Nat Med* 1999, **5:**512-517.

13. Sethi AK, Celentano DD, Gange SJ, Moore RD, Gallant JE: **Association between adherence to antiretroviral therapy and human immunodeficiency virus drug resistance.** *Clin Infect Dis* 2003, **37:**1112-1118.

14. Martins S, Ramos MJ, Fernandes PA: **The current status of the NNRTI family of antiretrovirals used in the HAART regime against HIV infection.** *Curr Med Chem* 2008, **15:**1083-1095.

15. Kuritzkes DR, Jacobson J, Powderly WG, Godofsky E, DeJesus E, Haas F, Reimann KA, Larson JL, Yarbough PO, Curt V, Shanahan WR, Jr.: **Antiretroviral activity of the anti-CD4 monoclonal antibody TNX-355 in patients infected with HIV type 1.** *J Infect Dis* 2004, **189:**286-291.

16. Dau B, Holodniy M: **Novel targets for antiretroviral therapy: clinical progress to date.** *Drugs* 2009, **69:**31-50.

17. Suzuki T, Yamamoto N, Nonaka M, Hashimoto Y, Matsuda G, Takeshima SN, Matsuyama M, Igarashi T, Miura T, Tanaka R, et al: **Inhibition of human immunodeficiency virus type 1 (HIV-1) nuclear import via Vpr-Importin alpha interactions as a novel HIV-1 therapy.** *Biochem Biophys Res Commun* 2009, **380:**838-843.

18. Li J, Tang S, Hewlett I, Yang M: **HIV-1 capsid protein and cyclophilin a as new targets for anti-AIDS therapeutic agents.** *Infect Disord Drug Targets* 2007, **7:**238-244.

19. Zhan P, Liu X, De Clercq E: **Blocking nuclear import of pre-integration complex: an emerging anti-HIV-1 drug discovery paradigm.** *Curr Med Chem* 2010, **17:**495-503.

20. Smith JL, Bu W, Burdick RC, Pathak VK: **Multiple ways of targeting APOBEC3-virion infectivity factor interactions for anti-HIV-1 drug development.** *Trends Pharmacol Sci* 2009, **30:**638-646.

21. Lori F, Foli A, Kelly LM, Lisziewicz J: **Virostatics: a new class of anti-HIV drugs.** *Curr Med Chem* 2007, **14:**233-241.

22. Jones KL, Smyth RP, Pereira CF, Cameron PU, Lewin SR, Jaworowski A, Mak J: **Early Events of HIV-1 Infection: Can Signaling be the Next Therapeutic Target?** *J Neuroimmune Pharmacol* 2011.

23. Greene WC, Debyser Z, Ikeda Y, Freed EO, Stephens E, Yonemoto W, Buckheit RW, Este JA, Cihlar T: **Novel targets for HIV therapy.** *Antiviral Res* 2008, **80:**251-265.

24. Coiras M, Lopez-Huertas MR, Sanchez del Cojo M, Mateos E, Alcami J: **Dual role of host cell factors in HIV-1 replication: restriction and enhancement of the viral cycle.** *AIDS Rev* 2010, **12:**103-112.

25. Malim MH, Emerman M: **HIV-1 accessory proteins--ensuring viral survival in a hostile environment.** *Cell Host Microbe* 2008, **3:**388-398.

26. Shen R, Richter HE, Smith PD: **Early HIV-1 target cells in human vaginal and ectocervical mucosa.** *Am J Reprod Immunol* 2010, **65:**261-267.

27. Montagnier L: **25 years after HIV discovery: prospects for cure and vaccine.** *Virology* 2010, **397:**248-254.

28. Warnke D, Barreto J, Temesgen Z: **Antiretroviral drugs.** *J Clin Pharmacol* 2007, **47:**1570-1579.

29. Ren J, Stammers DK: **Structural basis for drug resistance mechanisms for non-nucleoside inhibitors of HIV reverse transcriptase.** *Virus Res* 2008, **134:**157-170.

30. Wensing AM, van Maarseveen NM, Nijhuis M: **Fifteen years of HIV Protease Inhibitors: raising the barrier to resistance.** *Antiviral Res* 2010, **85:**59-74.

31. Dam E, Quercia R, Glass B, Descamps D, Launay O, Duval X, Krausslich HG, Hance AJ, Clavel F: **Gag mutations strongly contribute to HIV-1 resistance to protease inhibitors in highly drug-experienced patients besides compensating for fitness loss.** *PLoS Pathog* 2009, **5:**e1000345.

32. Pandey KK, Bera S, Vora AC, Grandgenett DP: **Physical trapping of HIV-1 synaptic complex by different structural classes of integrase strand transfer inhibitors.** *Biochemistry* 2010, **49:**8376-8387.

33. Ghosh RK, Ghosh SM, Chawla S: **Recent advances in antiretroviral drugs.** *Expert Opin Pharmacother* 2011, **12:**31-46.

34. Harris KS, Brabant W, Styrchak S, Gall A, Daifuku R: **KP-1212/1461, a nucleoside designed for the treatment of HIV by viral mutagenesis.** *Antiviral Res* 2005, **67:**1-9.

35. Budihas SR, Gorshkova I, Gaidamakov S, Wamiru A, Bona MK, Parniak MA, Crouch RJ, McMahon JB, Beutler JA, Le Grice SF: **Selective inhibition of HIV-1 reverse**

transcriptase-associated ribonuclease H activity by hydroxylated tropolones. *Nucleic Acids Res* 2005, **33:**1249-1256.

36. Sluis-Cremer N, Arion D, Parniak MA: **Destabilization of the HIV-1 reverse transcriptase dimer upon interaction with N-acyl hydrazone inhibitors.** *Mol Pharmacol* 2002, **62:**398-405.

37. Dandache S, Sevigny G, Yelle J, Stranix BR, Parkin N, Schapiro JM, Wainberg MA, Wu JJ: **In vitro antiviral activity and cross-resistance profile of PL-100, a novel protease inhibitor of human immunodeficiency virus type 1.** *Antimicrob Agents Chemother* 2007, **51:**4036-4043.

38. Nalam MN, Schiffer CA: **New approaches to HIV protease inhibitor drug design II: testing the substrate envelope hypothesis to avoid drug resistance and discover robust inhibitors.** *Curr Opin HIV AIDS* 2008, **3:**642-646.

39. Bannwarth L, Rose T, Dufau L, Vanderesse R, Dumond J, Jamart-Gregoire B, Pannecouque C, De Clercq E, Reboud-Ravaux M: **Dimer disruption and monomer sequestration by alkyl tripeptides are successful strategies for inhibiting wild-type and multidrug-resistant mutated HIV-1 proteases.** *Biochemistry* 2009, **48:**379-387.

40. Du L, Zhao YX, Yang LM, Zheng YT, Tang Y, Shen X, Jiang HL: **Symmetrical 1-pyrrolidineacetamide showing anti-HIV activity through a new binding site on HIV-1 integrase.** *Acta Pharmacol Sin* 2008, **29:**1261-1267.

41. Christ F, Voet A, Marchand A, Nicolet S, Desimmie BA, Marchand D, Bardiot D, Van der Veken NJ, Van Remoortel B, Strelkov SV, et al: **Rational design of small-molecule inhibitors of the LEDGF/p75-integrase interaction and HIV replication.** *Nat Chem Biol* 2010, **6:**442-448.

42. Hayouka Z, Rosenbluh J, Levin A, Loya S, Lebendiker M, Veprintsev D, Kotler M, Hizi A, Loyter A, Friedler A: **Inhibiting HIV-1 integrase by shifting its oligomerization equilibrium.** *Proc Natl Acad Sci U S A* 2007, **104:**8316-8321.

43. Rosenbluh J, Hayouka Z, Loya S, Levin A, Armon-Omer A, Britan E, Hizi A, Kotler M, Friedler A, Loyter A: **Interaction between HIV-1 Rev and integrase proteins: a basis for the development of anti-HIV peptides.** *J Biol Chem* 2007, **282:**15743-15753.

44. Blair WS, Cao J, Jackson L, Jimenez J, Peng Q, Wu H, Isaacson J, Butler SL, Chu A, Graham J, et al: **Identification and characterization of UK-201844, a novel inhibitor that interferes with human immunodeficiency virus type 1 gp160 processing.** *Antimicrob Agents Chemother* 2007, **51:**3554-3561.

45. Jiang Y, Liu X, De Clercq E: **New therapeutic approaches targeted at the late stages of the HIV-1 replication cycle.** *Curr Med Chem* 2011, **18:**16-28.

46. Temesgen Z, Feinberg JE: **Drug evaluation: bevirimat--HIV Gag protein and viral maturation inhibitor.** *Curr Opin Investig Drugs* 2006, **7:**759-765.

47. Emert-Sedlak L, Kodama T, Lerner EC, Dai W, Foster C, Day BW, Lazo JS, Smithgall TE: **Chemical library screens targeting an HIV-1 accessory factor/host cell kinase complex identify novel antiretroviral compounds.** *ACS Chem Biol* 2009, **4:**939-947.

48. Kamata M, Wu RP, An DS, Saxe JP, Damoiseaux R, Phelps ME, Huang J, Chen IS: **Cell-based chemical genetic screen identifies damnacanthal as an inhibitor of HIV-1 Vpr induced cell death.** *Biochem Biophys Res Commun* 2006, **348:**1101-1106.

49. Watanabe N, Nishihara Y, Yamaguchi T, Koito A, Miyoshi H, Kakeya H, Osada H: **Fumagillin suppresses HIV-1 infection of macrophages through the inhibition of Vpr activity.** *FEBS Lett* 2006, **580:**2598-2602.

50. Lee CW, Cao H, Ichiyama K, Rana TM: **Design and synthesis of a novel peptidomimetic inhibitor of HIV-1 Tat-TAR interactions: squaryldiamide as a new potential bioisostere of unsubstituted guanidine.** *Bioorg Med Chem Lett* 2005, **15:**4243-4246.

51. Wolff B, Sanglier JJ, Wang Y: **Leptomycin B is an inhibitor of nuclear export: inhibition of nucleo-cytoplasmic translocation of the human immunodeficiency virus type 1 (HIV-1) Rev protein and Rev-dependent mRNA.** *Chem Biol* 1997, **4:**139-147.

52. Tavassoli A, Lu Q, Gam J, Pan H, Benkovic SJ, Cohen SN: **Inhibition of HIV budding by a genetically selected cyclic peptide targeting the Gag-TSG101 interaction.** *ACS Chem Biol* 2008, **3:**757-764.

53. Domenech R, Abian O, Bocanegra R, Correa J, Sousa-Herves A, Riguera R, Mateu MG, Fernandez-Megia E, Velazquez-Campoy A, Neira JL: **Dendrimers as potential inhibitors of the dimerization of the capsid protein of HIV-1.** *Biomacromolecules* 2010, **11:**2069-2078.

54. Rice WG, Supko JG, Malspeis L, Buckheit RW, Jr., Clanton D, Bu M, Graham L, Schaeffer CA, Turpin JA, Domagala J, et al: **Inhibitors of HIV nucleocapsid protein zinc fingers as candidates for the treatment of AIDS.** *Science* 1995, **270:**1194-1197.

55. Waheed AA, Ablan SD, Soheilian F, Nagashima K, Ono A, Schaffner CP, Freed EO: **Inhibition of human immunodeficiency virus type 1 assembly and release by the cholesterol-binding compound amphotericin B methyl ester: evidence for Vpu dependence.** *J Virol* 2008, **82:**9776-9781.

56. Cen S, Peng ZG, Li XY, Li ZR, Ma J, Wang YM, Fan B, You XF, Wang YP, Liu F, et al: **Small molecular compounds inhibit HIV-1 replication through specifically stabilizing APOBEC3G.** *J Biol Chem* 2010, **285:**16546-16552.

57. Kulkosky J, Culnan DM, Roman J, Dornadula G, Schnell M, Boyd MR, Pomerantz RJ: **Prostratin: activation of latent HIV-1 expression suggests a potential inductive adjuvant therapy for HAART.** *Blood* 2001, **98:**3006-3015.

58. Perez OD, Nolan GP, Magda D, Miller RA, Herzenberg LA: **Motexafin gadolinium (Gd-Tex) selectively induces apoptosis in HIV-1 infected CD4+ T helper cells.** *Proc Natl Acad Sci U S A* 2002, **99:**2270-2274.

59. Veselovsky AV, Archakov AI: **Inhibitors of protein-protein interactions as potential drugs.** *Current Computer-Aided Drug Design* 2007, **3:**51-58.

60. Kwak YT, Raney A, Kuo LS, Denial SJ, Temple BR, Garcia JV, Foster JL: **Self-association of the Lentivirus protein, Nef.** *Retrovirology* 2010, **7:**77.

61. Frankel AD, Chen L, Cotter RJ, Pabo CO: **Dimerization of the tat protein from human immunodeficiency virus: a cysteine-rich peptide mimics the normal metal-linked dimer interface.** *Proc Natl Acad Sci U S A* 1988, **85:**6297-6300.

62. DiMattia MA, Watts NR, Stahl SJ, Rader C, Wingfield PT, Stuart DI, Steven AC, Grimes JM: **Implications of the HIV-1 Rev dimer structure at 3.2 A resolution for multimeric binding to the Rev response element.** *Proc Natl Acad Sci U S A* 2010, **107:**5810-5814.

63. Miller JH, Presnyak V, Smith HC: **The dimerization domain of HIV-1 viral infectivity factor Vif is required to block virion incorporation of APOBEC3G.** *Retrovirology* 2007, **4:**81.

64. Paxton W, Connor RI, Landau NR: **Incorporation of Vpr into human immunodeficiency virus type 1 virions: requirement for the p6 region of gag and mutational analysis.** *J Virol* 1993, **67:**7229-7237.

65. Cardinale D, Salo-Ahen OM, Ferrari S, Ponterini G, Cruciani G, Carosati E, Tochowicz AM, Mangani S, Wade RC, Costi MP: **Homodimeric enzymes as drug targets.** *Curr Med Chem* 2010, **17:**826-846.

66. Arkin MR, Wells JA: **Small-molecule inhibitors of protein-protein interactions: progressing towards the dream.** *Nat Rev Drug Discov* 2004, **3:**301-317.

67. Luque I, Freire E: **Structural stability of binding sites: consequences for binding affinity and allosteric effects.** *Proteins* 2000, **Suppl 4:**63-71.

68. **Protein-protein interactions in drug discovery: another piece of the complex drug discovery process explained.** In *Genetic Engineering & Biotechnology News*, vol. 25. pp. 1; 2005:1.

69. Kerppola TK: **Visualization of molecular interactions using bimolecular fluorescence complementation analysis: characteristics of protein fragment complementation.** *Chem Soc Rev* 2009, **38:**2876-2886.

70. Schaferling M, Nagl S: **Forster resonance energy transfer methods for quantification of protein-protein interactions on microarrays.** *Methods Mol Biol* 2011, **723:**303-320.

71. Haupts U, Rudiger M, Pope AJ: **Macroscopic versus microscopic fluorescence techniques in (ultra)-high throughput screening.** *Drug Discov Today: HTS Supplement* 2000, **1**.

72. Guner O, Clement O, Kurogi Y: **Pharmacophore modeling and three dimensional database searching for drug design using catalyst: recent advances.** *Curr Med Chem* 2004, **11:**2991-3005.

73. Orita M, Ohno K, Warizaya M, Amano Y, Niimi T: **Lead generation and examples opinion regarding how to follow up hits.** *Methods Enzymol* 2011, **493:**383-419.

74. Potashman MH, Duggan ME: **Covalent modifiers: an orthogonal approach to drug design.** *J Med Chem* 2009, **52:**1231-1246.

75. Bull HG, Garcia-Calvo M, Andersson S, Baginsky WF, Chan HK, Ellsworth DE, Miller RR, Stearns RA, Bakshi RK, Rasmusson GH, et al: **Mechanism-based inhibition of human steroid 5α-reductase by finasteride: enyzme-catalyzed formation of NADP-dihydrofinasteride, a potent bisubstrate analog inhibitor.** *J Am Chem Soc* 1996, **118:**2359-2365.

76. Fukumori T, Akari H, Yoshida A, Fujita M, Koyama AH, Kagawa S, Adachi A: **Regulation of cell cycle and apoptosis by human immunodeficiency virus type 1 Vpr.** *Microbes Infect* 2000, **2:**1011-1017.

77. Ayyavoo V, Mahboubi A, Mahalingam S, Ramalingam R, Kudchodkar S, Williams WV, Green DR, Weiner DB: **HIV-1 Vpr suppresses immune activation and apoptosis through regulation of nuclear factor kappa B.** *Nat Med* 1997, **3:**1117-1123.

78. Cheng X, Mukhtar M, Acheampong EA, Srinivasan A, Rafi M, Pomerantz RJ, Parveen Z: **HIV-1 Vpr potently induces programmed cell death in the CNS in vivo.** *DNA Cell Biol* 2007, **26:**116-131.

79. Majumder B, Janket ML, Schafer EA, Schaubert K, Huang XL, Kan-Mitchell J, Rinaldo CR, Jr., Ayyavoo V: **Human immunodeficiency virus type 1 Vpr impairs dendritic cell maturation and T-cell activation: implications for viral immune escape.** *J Virol* 2005, **79:**7990-8003.

80. Majumder B, Venkatachari NJ, Srinivasan A, Ayyavoo V: **HIV-1 mediated immune pathogenesis: spotlight on the role of viral protein R (Vpr).** *Curr HIV Res* 2009, **7:**169-177.

81. Tungaturthi PK, Sawaya BE, Singh SP, Tomkowicz B, Ayyavoo V, Khalili K, Collman RG, Amini S, Srinivasan A: **Role of HIV-1 Vpr in AIDS pathogenesis: relevance and implications of intravirion, intracellular and free Vpr.** *Biomed Pharmacother* 2003, **57:**20-24.

82. Venkatachari NJ, Walker LA, Tastan O, Le T, Dempsey TM, Li Y, Yanamala N, Srinivasan A, Klein-Seetharaman J, Montelaro RC, Ayyavoo V: **Human immunodeficiency virus type 1 Vpr: oligomerization is an essential feature for its incorporation into virus particles.** *Virol J* 2010, **7:**119.

83. Nitahara-Kasahara Y, Kamata M, Yamamoto T, Zhang X, Miyamoto Y, Muneta K, Iijima S, Yoneda Y, Tsunetsugu-Yokota Y, Aida Y: **Novel nuclear import of Vpr promoted by importin alpha is crucial for human immunodeficiency virus type 1 replication in macrophages.** *J Virol* 2007, **81:**5284-5293.

84. Popov S, Rexach M, Zybarth G, Reiling N, Lee MA, Ratner L, Lane CM, Moore MS, Blobel G, Bukrinsky M: **Viral protein R regulates nuclear import of the HIV-1 pre-integration complex.** *EMBO J* 1998, **17:**909-917.

85. Agostini I, Navarro JM, Rey F, Bouhamdan M, Spire B, Vigne R, Sire J: **The human immunodeficiency virus type 1 Vpr transactivator: cooperation with promoter-bound activator domains and binding to TFIIB.** *J Mol Biol* 1996, **261:**599-606.

86. Aida Y, Matsuda G: **Role of Vpr in HIV-1 nuclear import: therapeutic implications.** *Curr HIV Res* 2009, **7:**136-143.

87. Zhao RY, Li G, Bukrinsky MI: **Vpr-Host Interactions During HIV-1 Viral Life Cycle.** *J Neuroimmune Pharmacol* 2011.

88. Chen R, Le Rouzic E, Kearney JA, Mansky LM, Benichou S: **Vpr-mediated incorporation of UNG2 into HIV-1 particles is required to modulate the virus mutation rate and for replication in macrophages.** *J Biol Chem* 2004, **279:**28419-28425.

89. Zhao LJ, Wang L, Mukherjee S, Narayan O: **Biochemical mechanism of HIV-1 Vpr function. Oligomerization mediated by the N-terminal domain.** *J Biol Chem* 1994, **269:**32131-32137.

90. Pandey RC, Datta D, Mukerjee R, Srinivasan A, Mahalingam S, Sawaya BE: **HIV-1 Vpr: a closer look at the multifunctional protein from the structural perspective.** *Curr HIV Res* 2009, **7:**114-128.

91. Morellet N, Roques BP, Bouaziz S: **Structure-function relationship of Vpr: biological implications.** *Curr HIV Res* 2009, **7:**184-210.

92. Fritz JV, Dujardin D, Godet J, Didier P, De Mey J, Darlix JL, Mely Y, de Rocquigny H: **HIV-1 Vpr oligomerization but not that of Gag directs the interaction between Vpr and Gag.** *J Virol* 2010, **84:**1585-1596.

93. Sherman MP, de Noronha CM, Eckstein LA, Hataye J, Mundt P, Williams SA, Neidleman JA, Goldsmith MA, Greene WC: **Nuclear export of Vpr is required for efficient replication of human immunodeficiency virus type 1 in tissue macrophages.** *J Virol* 2003, **77:**7582-7589.

94. Zhao Y, Yu M, Chen M, Elder RT, Yamamoto A, Cao J: **Pleiotropic effects of HIV-1 protein R (Vpr) on morphogenesis and cell survival in fission yeast and antagonism by pentoxifylline.** *Virology* 1998, **246:**266-276.

95. Yao XJ, Lemay J, Rougeau N, Clement M, Kurtz S, Belhumeur P, Cohen EA: **Genetic selection of peptide inhibitors of human immunodeficiency virus type 1 Vpr.** *J Biol Chem* 2002, **277:**48816-48826.

96. Schafer EA, Venkatachari NJ, Ayyavoo V: **Antiviral effects of mifepristone on human immunodeficiency virus type-1 (HIV-1): targeting Vpr and its cellular partner, the glucocorticoid receptor (GR).** *Antiviral Res* 2006, **72:**224-232.

97. Hagiwara K, Murakami T, Xue G, Shimizu Y, Takeda E, Hashimoto Y, Honda K, Kondoh Y, Osada H, Tsunetsugu-Yokota Y, Aida Y: **Identification of a novel Vpr-binding compound that inhibits HIV-1 multiplication in macrophages by chemical array.** *Biochem Biophys Res Commun* 2010, **403:**40-45.

98. Ong EB, Watanabe N, Saito A, Futamura Y, Abd El Galil KH, Koito A, Najimudin N, Osada H: **VIPIRININ, a coumarin-based HIV-1 VPR inhibitor, interacts with a hydrophobic region of VPR.** *J Biol Chem* 2011.

99. Guan H, Kiss-Toth E: **Advanced technologies for studies on protein interactomes.** *Adv Biochem Eng Biotechnol* 2008, **110:**1-24.

100. Remy I, Michnick SW: **A highly sensitive protein-protein interaction assay based on Gaussia luciferase.** *Nat Methods* 2006, **3:**977-979.

101. Johnsson N, Varshavsky A: **Split ubiquitin as a sensor of protein interactions in vivo.** *Proc Natl Acad Sci U S A* 1994, **91:**10340-10344.

102. Pelletier JN, Campbell-Valois FX, Michnick SW: **Oligomerization domain-directed reassembly of active dihydrofolate reductase from rationally designed fragments.** *Proc Natl Acad Sci U S A* 1998, **95:**12141-12146.

103. Kerppola TK: **Bimolecular fluorescence complementation (BiFC) analysis as a probe of protein interactions in living cells.** *Annu Rev Biophys* 2008, **37:**465-487.

104. Zhang JH, Chung TD, Oldenburg KR: **A Simple Statistical Parameter for Use in Evaluation and Validation of High Throughput Screening Assays.** *J Biomol Screen* 1999, **4:**67-73.

105. Shun TY, Lazo JS, Sharlow ER, Johnston PA: **Identifying actives from HTS data sets: practical approaches for the selection of an appropriate HTS data-processing method and quality control review.** *J Biomol Screen* 2011, **16:**1-14.

106. Mepham SO, Bland RM, Newell ML: **Prevention of mother-to-child transmission of HIV in resource-rich and -poor settings.** *BJOG* 2011, **118:**202-218.

107. Camarasa MJ, Velazquez S, San-Felix A, Perez-Perez MJ, Gago F: **Dimerization inhibitors of HIV-1 reverse transcriptase, protease and integrase: a single mode of inhibition for the three HIV enzymes?** *Antiviral Res* 2006, **71:**260-267.

108. Piller SC, Caly L, Jans DA: **Nuclear import of the pre-integration complex (PIC): the Achilles heel of HIV?** *Curr Drug Targets* 2003, **4:**409-429.

109. Agler M, Prack M, Zhu Y, Kolb J, Nowak K, Ryseck R, Shen D, Cvijic ME, Somerville J, Nadler S, Chen T: **A high-content glucocorticoid receptor translocation assay for compound mechanism-of-action evaluation.** *J Biomol Screen* 2007, **12:**1029-1041.

110. Bianchi BR, Moreland RB, Faltynek CR, Chen J: **Application of large-scale transiently transfected cells to functional assays of ion channels: different targets and assay formats.** *Assay Drug Dev Technol* 2007, **5:**417-424.

111. Chen J, Lake MR, Sabet RS, Niforatos W, Pratt SD, Cassar SC, Xu J, Gopalakrishnan S, Pereda-Lopez A, Gopalakrishnan M, et al: **Utility of large-scale transiently transfected cells for cell-based high-throughput screens to identify transient receptor potential channel A1 (TRPA1) antagonists.** *J Biomol Screen* 2007, **12:**61-69.

112. Kiessling A, Sperl B, Hollis A, Eick D, Berg T: **Selective inhibition of c-Myc/Max dimerization and DNA binding by small molecules.** *Chem Biol* 2006, **13:**745-751.

113. Chen TS, Reinke AW, Keating AE: **Design of Peptide Inhibitors That Bind the bZIP Domain of Epstein-Barr Virus Protein BZLF1.** *J Mol Biol* 2011.

114. Mason JM, Muller KM, Arndt KM: **Positive aspects of negative design: simultaneous selection of specificity and interaction stability.** *Biochemistry* 2007, **46:**4804-4814.